Analytical Methods

Accepted Manuscript

This is an *Accepted Manuscript*, which has been through the RSC Publishing peer review process and has been accepted for publication.

Accepted Manuscripts are published online shortly after acceptance, which is prior to technical editing, formatting and proof reading. This free service from RSC Publishing allows authors to make their results available to the community, in citable form, before publication of the edited article. This *Accepted Manuscript* will be replaced by the edited and formatted *Advance Article* as soon as this is available.

To cite this manuscript please use its permanent Digital Object Identifier (DOI®), which is identical for all formats of publication.

More information about *Accepted Manuscripts* can be found in the **Information for Authors**.

Please note that technical editing may introduce minor changes to the text and/or graphics contained in the manuscript submitted by the author(s) which may alter content, and that the standard **Terms & Conditions** and the **ethical guidelines** that apply to the journal are still applicable. In no event shall the RSC be held responsible for any errors or omissions in these *Accepted Manuscript* manuscripts or any consequences arising from the use of any information contained in them.

Rhoeo discolor leaf extract as a novel immobilizing matrix for the fabrication of electrochemical glucose and hydrogen peroxide biosensor

Seetharamaiah Nandini,[a] Seetharamaiah Nalini,[a] Sangaraju Shanmugam,[b] P Niranjana,[c] Jose Savio Melo[d*] and Gurukar Shivappa Suresh[a*]

[a]*Department of Chemistry and Research Centre, N.M.K.R.V. College for Women, Jayanagar, Bangalore 560 011, India*

[b]*Department of Energy Systems and Engineering, Daegu Gyeongbuk Institute of Science and Technology, Daegu 711-873, Republic of Korea*

[c]*Department of Biochemistry, Kuvempu University, Shankarghatta, Shimoga 577451, India*

[d]*Nuclear Agriculture and Biotechnology Division, Bhabha Atomic Research Centre, Mumbai 400 085, India*

**Corresponding author*

Telephone: 91-80-26654920

Fax no: 91-80-22453665

E-mail: sureshssmrv@yahoo.co.in (G.S. Suresh),

jsmelo@barc.gov.in (J.S. Melo)

Abstract

A novel natural immobilizing matrix for the immobilization of glucose oxidase (GOx) and horseradish peroxidase (HRP) is being presented through this article. The electrochemical biosensor was constructed by immobilizing the enzymes on *Rhoeo discolor* (Rd) leaf extract with 2.5% Gluteraldehyde (GLD) on functionalized multiwalled carbon nanotubes (f-MWCNTs) modified Graphite (Gr) electrode. The Gr/f-MWCNTs/(Rd-GLD)/GOx and Gr/f-MWCNTs/(Rd-GLD)/HRP biosensors showed excellent electrocatalytic activity as far as the detection of glucose and hydrogen peroxide was concerned. The physical morphology of the biosensors was studied using SEM and EDX. The electrochemical performance of the proposed biosensors was evaluated using cyclic voltammetry, differential pulse voltammetry and chronoamperometry. The effects of experimental variables such as pH, temperature, and applied potential on current response of the biosensors were studied and optimized. The Gr/f-MWCNTs/(Rd-GLD)/GOx biosensor exhibited a rapid response time of less than 5 s, displayed a wide linear range of 0.5 to 28.5 mM, showed a low detection limit of 0.16 μM and revealed a high sensitivity of 15 μA mM^{-1} cm^{-2} for glucose. Similarly Gr/f-MWCNTs/(Rd-GLD)/HRP biosensor showed a fast response time of 3 s, a good linear range of 0.2 to 6.8 mM with 0.01 μM of the detection limit and an exceptional sensitivity of 2.1 mA mM^{-1} cm^{-2} for hydrogen peroxide. Subsequently, the practical applicability of the glucose biosensor for the analysis of glucose in *Eleusine coracana* wine and tender coconut water was examined while the Gr/f-MWCNTs/(Rd-GLD)/HRP modified electrode was tested for the determination of H_2O_2 in herbal bleach. In addition, the biosensors displayed long term stability, anti-interference ability and good reproducibility.

1. Introduction

Biosensor is a term used for a sensing device that comprises a biological detection component in close proximity with an appropriate transducer, which is capable of translating the biological detection reaction or the biocatalytic system into an assessable signal. The most commonly used biological components in biosensors are enzymes. Several enzymes such as glucose oxidase (GOx), horseradish peroxidase (HRP), cholesterol oxidase (ChOx), etc., have been successfully immobilized and employed in the analysis of glucose,[1] hydrogen peroxide[2] (H_2O_2) and cholesterol[3] respectively. Various strategies have been developed for the determination of these target analytes, such as titrimetry,[4] flurometry,[5] spectrometry,[6] chemiluminescence,[7] and electrochemical enzyme biosensors.[8] Among these methods electrochemical enzyme biosensors have been extensively used due to their low cost, efficiency, simplicity, intrinsic sensitivity to electrochemical transduction process and excellent selectivity of biological recognition element. The idea of integrating the specificity of a biological system with the simplicity and sensitivity of electrochemical transduction led to the construction of the first enzyme electrode by Leland C. Clark to detect glucose.[9] Since then the development of an ideal, cheap, accurate, easy to handle glucose biosensor has remained the prime focus of many researchers. This is also because of its importance in the diagnosis and management of diabetes mellitus. The advancement achieved in this direction is predominantly evident in the development of amperometric glucose biosensors based on GOx that generates H_2O_2 in the presence of dioxygen and glucose. In these devices either the formation of H_2O_2[10] or the consumption of dioxygen[11] is monitored on the electrode surface. GOx (E.C.1.1.3.4) is a homodimer with a molecular weight of 186 kD. It has two molecules of strongly bound flavine adenine dinucleotide (FAD) which is a redox prosthetic group.[12] HRP (E.C. 1.11.1.7) is one of the most widely used heme-containing enzymes for the detection of H_2O_2.[13] The electro-catalytic activity of HRP is based on a mechanism in which

H_2O_2 oxidises the co-factor protohemin IX, which consecutively undergoes reduction to facilitate prolonging the catalytic cycle.[14] However from a bio-electrochemical point of view, well-defined electrochemical behaviour of the flavoprotein-GOx or heme moiety in HRP enzyme is rendered very complicated because of the deep embedding of the electrochemical prosthetic groups within the protein structure.[15] Therefore, enzyme immobilization is a crucial factor in accomplishing high performance of the biosensor with direct electron tunnelling between the enzyme's active site and the electrode surface. Significant efforts have been made to obtain direct electron transfer by implementing novel biocompatible matrix and developing an appropriate immobilization method to retain enzyme activity and to have freedom from fouling by endogenous macromolecules and to achieve low interference from reducing agents. Many publications concerning the enzyme immobilization methods have been reported which include electropolymerisation,[16] sol-gels,[17]self-assembled monolayers,[18] polymer entrapment,[19] covalent linking,[20] physical adsorption[21] and cross-linking.[22] Immobilization by physical adsorption is simple and entails reversible surface interaction between enzyme and supporting material. It has many advantages like prevention of denaturation of the enzyme, which is also a cheap and quick method. Disappointingly the major problem of this method is the faster leakage of the enzyme during reaction, thereby contaminating the substrate which results in short-life time of the biosensor. Hence the biosensor usually lacks reusability. However this problem can be significantly overcome by using adsorption followed by cross-linking which increases reusability and stability of the immobilized enzyme. GLD is widely used as a cross-linking agent that can prevent leaching out of the immobilized enzymes. Meanwhile various supporting materials have also been explored such as organic films, synthetic and natural polymers, nafion, nanometre materials, screen printed films, polyelectrolyte and rigid composite based on graphite, Teflon and inorganic matrices. Amongst them natural polymers such as egg shell membrane,[23]

collagen,[24] silk,[25] bamboo inner shell membrane[26] and onion bulb scale[27] have been elegantly utilized as matrices for enzyme immobilization. It is essential to state that there is still intensive research going on in the development of newer methods and in the incorporation of novel materials for the construction of desirable biocomposite nanostructures. Ever since carbon nanotubes (CNTs) were discovered,[28] there has been a focus of interest for many scientists owing to their exceptional properties such as high tensile strength, high surface area, excellent thermal, chemical properties and admirable biocompatibility.[29-31] CNTs can be classified as single-walled nanotubes (SWCNTs) or as multi-walled nanotubes (MWCNTs). MWCNTs have a fast electron transfer rate and enhanced electrical conductivity compared to SWCNTs. Nowadays, MWCNTs have been extensively utilized in the fabrication of electrochemical biosensors due to their tremendous electrocatalytic activity and antifouling properties.[32] *Rhoeo discolor* (Rd) is a plant that belongs to *Commelinaceae* family and is used in conventional medicine. The phytochemical evaluation of the plant has shown the presence of polyphenols (flavonoids, anthocyannins), saponnins, carotenoids, waxes, terpenoids, etc.[33] The extracts of the plant have been incorporated in cosmetics.[34] The bioactive components like polyphenols produce quinones[35] on oxidation which generally increase the kinetics of electron transfer by implementing electrical contact between the redox centre of the enzyme and the electrode surface.[36] In addition, the polyphenols have been proved to be exceptionally helpful in imparting high selectivity by accelerating the degradation of highly active electrochemical interferents.[37] The aim of the present research investigation is to use Rd leaf extract as a matrix for enzyme immobilization in the development of electrochemical biosensor. This new material has many fascinating features like inertness to microbes; available from renewable source; highly cost effective and has elevated selectivity which diminishes the access of interference substances to the electrode surface. In addition, it has an admirable thermal tolerance, an exceptional chemical resistance and an excellent electron

transfer ability so as to limit the use of electron mediators. Consequently preventing the tedious fabrication procedure required for the co-immobilization of enzyme and electron mediators. Therefore Rd may be an ideal bio-platform for enzyme immobilization and can provide a biocompatible microenvironment.

Herein, we propose a simple and novel strategy of application of a leaf extract as an enzyme immobilization matrix in biosensor fabrication. To the best of our knowledge there has been no evidence documented from the use of Rd leaf in biosensor application. In the current work, the unique properties of Rd leaf were successfully explored for the first time for the immobilization of GOx through cross-linking with 2.5% GLD onto f-MWCNTs modified Gr electrode. Surface characterization and chemical composition of the modified electrodes were evaluated using SEM and EDX. The electrochemical behaviour of the electrode towards glucose detection was studied using CV, DPV and chronoamperometry. The modified electrodes showed excellent electrocatlytic activity towards the analyte with excellent linear range, fast response time, reproducibility, anti-interference ability and stability. The attractive performance of the biosensor fabricated using easily available, evergreen, non toxic Rd leaf motivated us to further extend the study to incorporate HRP for the development of H_2O_2 biosensor.

2. Experimental details

2.1 Reagents and materials

GOx, type X-S from *Aspergillus niger* lyophilized powder 50 kU, HRP (250U), MWCNTs, ascorbic acid (AA), dopamine (DA), acetaminophen (ACT) and uric acid (UA) were purchased from Sigma Aldrich, USA. GOx suspension was prepared by dissolving the lyophilized enzyme in buffer solution of pH 4 to a final concentration of 5 mg mL^{-1} while HRP suspension was prepared by dissolving the enzyme in pH 7 buffer solution to the same

5 mg mL^{-1} concentration. PK-3 electrode polishing kit (0.05 μm aqueous polishing alumina and 1 μm polishing diamond) was procured from BAS Inc. Tokyo, Japan. MWCNTs have a tendency to aggregate in most of the solvents owing to the van der Waals forces. To overcome this limitation functionalization of MWCNTs was carried out to increase the solubility and dispersibility in solution. In the present approach, MWCNTs were refluxed with con. HNO_3 at 70 ˚C for 5 h, washed several times with double distilled water, until the washing became neutral and finally dried at 85 ˚C under vacuum. This resulted in carboxylic acid functionalized MWCNTs (f-MWCNTs). 25 % GLD solution was procured from Central Drug House (India). Glucose and 30 % H_2O_2 were obtained from Merck. Blooming plants of Rd were collected from local area washed with running water and further cleaned by ultrasonication. Fresh leaves of Rd were cut in fragments (400 mg) and extracted with 300 μL of 2.5 % GLD until a solid paste has formed. This (2.5 %) concentration of GLD was found to be optimum. This was determined using trial and error based on reaction time, pH, concentration of enzyme and reagent. This concentration didn't have any adverse or toxic effects on the enzyme as the enzyme maintained stability throughout the experiments. This Rd casting solution was used as a matrix for enzyme immobilization. The phenolic content of the fresh Rd leaf was calculated using Gallic acid as the standard and the results as expressed as mg L^{-1} Gallic acid equivalents (GAE). The amount of total phenol in the Rd leaf was found to be 2080 mg GAE L^{-1} which was close to the reported value 2100±17 mg GAE L^{-1}.[38] Phosphate buffer saline (PBS) was prepared from stock solution of 0.1 M K_2HPO_4, 0.1 M KH_2PO_4 and 0.1 M KCl. pH was adjusted using 0.5 M HCl and 0.5 M NaOH. All other chemicals used were of analytical reagent grade, unless otherwise mentioned, and were used without further purification.

2.2 Electrochemical measurements

Cyclic voltammetry (CV), differential pulse voltammetry (DPV) and electrochemical impedance spectroscopy (EIS) were carried out with Versa stat 3 (Princeton Applied Research, USA).The impedance spectra were further examined by using a stimulated programme of Zsimp Win version 3.20. The electrochemical quartz crystal microbalance (EQCM) measurements were performed using CH instruments Inc. Scanning Electron Microscopy (SEM) and Energy Dispersive Analysis of X-rays (EDX) mapping measurements were done using FE-SEM, model (Hitachi S-4800 II) with an accelerating voltage of 5 kV. Temperature measurements were carried out using Equitron®, digital temperature controller equipped with stirred water bath. All experiments were done in a conventional three electrode electrochemical cell with bare Gr or enzyme modified electrode as working electrode, saturated calomel electrode (SCE) as reference electrode and platinum wire as auxiliary electrode. The working electrode for EQCM was a 7.99 MHz AT-cut quartz crystal (diameter 13.7 mm) coated with a gold electrode (diameter 5.1 mm) obtained from CH instruments Inc.

2.3 Preparation of enzyme modified electrode

An electrode was made by inserting a Gr rod of 6 mm diameter into the 10 mm diameter hollow Teflon cylinder with a recessed depth of 0.5 mm. Electrical contact was made by using a threaded aluminium rod that was fitted into the hollow Teflon cylinder in such a manner that only 0.5 mm of the Gr surface was exposed to the solution. Before placing the Gr rod into the hollow cylinder its surface was polished to get a mirror shiny surface using PK-3 electrode polishing kit. It was then ultrasonicated for several minutes and rinsed with double distilled water followed by drying. A stock solution of 2 mg mL^{-1} f-MWCNTs was prepared with the aid of ultrasonication by dispersing 10 mg of f-MWCNTs in 5 mL of double distilled water to get a stable black suspension. 5 µL of f-MWCNTs dispersion was dropped onto the surface of Gr electrode and allowed to air dry to form uniform coating of

f-MWCNTs. Schematic illustration of the fabrication process is given in Fig. 1. For the construction of glucose biosensor a 10 μL of the Rd casting solution was dropped onto the surface of the Gr/f-MWCNTs electrode and spread uniformly followed by incubation at room temperature. Subsequently the electrode was modified by dropping 10 μL GOx suspensions (5 mg mL^{-1}) to form a coating on the electrode surface and then dried at 4 ˚C in the refrigerator for 30 min. The Gr/f-MWCNTs/(Rd-GLD)/HRP electrode was prepared by the same procedure as briefed above except that instead of GOx, HRP was dropped and incubated at 4 ˚C for 30 min. The resulting enzyme electrode Gr/f-MWCNTs/(Rd-GLD)/GOx and (Gr/f-MWCNTs/(Rd-GLD)/HRP were rinsed thoroughly with pure water before use in order to remove any unbound or loosely attached enzymes. The prepared electrodes were stored at 4 ˚C when not in use. For comparative studies bare Gr, Gr/f-MWCNTs and Gr/f-MWCNTs/Rd-GLD was prepared in the similar manner.

3. Results and Discussions

3.1 Physical characterization of the modified electrodes using SEM and EDX

The physical morphology of the surface of the electrodes during stepwise modification was evaluated using SEM. Fig 2A depicts a network of tubular structure of f-MWCNTs twining homogeneously throughout the surface of the Gr which could be attributed to optimum dispersion of f-MWCNTs in water via sonication. It is observed that the morphology of Gr/f-MWCNTs/Rd- GLD (Fig. 2B) is completely altered exhibiting undetectable f-MWCNTs with squashy appearance. Comparatively, the SEM images of the Gr/f-MWCNTs/(Rd-GLD)/GOx (Fig 2C) and Gr/f-MWCNTs/(Rd-GLD)/HRP (Fig. 2D) composites illustrate small globules of enzyme molecules with the disappearance of the squashy structure implying that the Rd matrix acts as a supporting matrix that can absorb the enzymes in its native structure, meanwhile retaining the enzyme activity which can be proved by electrochemical experiments.

As a point of comparison, EDX was also used as an appropriate tool to determine the chemical composition of the modified electrodes. The EDX analysis which was carried out on various portions of the electrode surface is tabulated in the inset of Fig. 3(A-D). As can be seen in Fig. 3A, the modification of Gr surface with f-MWCNTs was confirmed by the appearance of distinct C, O and N peaks indicating the carbon and oxygen containing functional groups. When the Rd leaf extract was applied to construct the Gr/f-MWCNTs/Rd-GLD electrode (Fig. 3B), the EDX depicts the presence of C, O, Mg and Cl peaks as the prominent peaks of the composite. The C, O corresponds to f-MWCNTs while the Mg peak may be due to the porphyrin ring of chlorophyll present in the Rd extract. Interestingly, the EDX results presented in Fig. 3C exhibits well defined C, O, Cl, Mg and P elements validating the successful immobilization of GOx possible through the presence of P peak which is an ingredient of a FAD redox prosthetic group of the enzyme. However, the EDX recorded for the Gr/f-MWCNTs/(Rd-GLD)/HRP (Fig. 3D) revealed the presence of C, O, Mg, Cl along with Ca peaks. The Ca peak is assumed to exist virtually due to the endogenous calcium ions present in HRP thus establishing the immobilization of enzyme.

3.2 Electrochemical characterization of the enzyme modified electrode using CV and EIS

CV of redox couple ferricyanide is a valuable and suitable technique to examine the barrier of the modified electrodes. Therefore CV was performed to investigate the features of surface modified electrodes in the presence of 5 mM equimolar electrochemical redox probe $Fe(CN)_6^{3-/4-}$ in PBS pH 7. The redox behaviour of $Fe(CN)_6^{3-/4-}$ at the bare Gr electrode was studied and compared with the other modified electrodes after each modifying step. From, Fig. 4A (a) it can be clearly seen that a pair of well defined quarsi-reversible redox peaks with a peak-potential separation (ΔE_p) of 181 mV was exhibited at the bare Gr electrode.

Comparatively, the CV of the redox couple on Gr/f-MWCNTs [Fig. 4A (b)] reveals an increment in oxidation and reduction peak current with a ΔE_p of 150 mV which is due to the presence of highly conductive f-MWCNTs, that increase the surface of the electrode and facilitate the electron exchange between the electrode and the electrochemical probe. Nonetheless, the Gr/f-MWCNTs/Rd-GLD electrode as observed in Fig. 4A (c) demonstrates an increased ΔE_p (=213 mV) and a remarkable current enhancement with a 1.5 fold and 1 fold higher oxidation and reduction peak current respectively as compared to the bare Gr electrode. The reason for rapid electron transfer may be due to the presence of bioactive components like polyphenols which on oxidation produce quinones which generally increase the kinetics of electron transfer. Relatively, after modification with enzymes the faradic current at the Gr/f-MWCNTs/(Rd-GLD)/GOx [Fig. 4A (d)] and Gr/f-MWCNTs/(Rd-GLD)/HRP [Fig. 4A (e)] electrodes decreased with ΔE_p of 208 mV and 190 mV respectively indicating that the GOx and HRP are weak barriers to $Fe(CN)_6^{3-/4-}$ ion penetration. This is attributed to the negative charge of GOx and HRP that hinders the diffusion of the negatively charged redox probe towards the electrode surface.

The information on the electrical characteristics at the electrode/electrolyte interface of the modified electrode was assessed using EIS measurements. A formal potential as estimated from CVs during stepwise modification of the electrode surface was used for the measurement of impedance. Fig. 4B shows distinctive Nyquist impedance plots recorded in the frequency range of 100 kHz to 10 Hz. The results in the Fig. 4B (a) indicates that the charge transfer resistance (R_{ct}184 Ω) of bare Gr electrode is considerably larger when compared with f-MWCNTs, [Fig. 4B (b)] justifying the interpretation that the introduction of the f-MWCNTs would significantly increase the surface area of the electrode, which makes the electron transfer much larger and conversely smaller R_{ct} (44.01Ω). Following the further

modification of the electrode with Rd leaf extract, the R_{ct} (16.98Ω) value of the Gr/f-MWCNTs/Rd-GLD electrode [Fig. 4B (c)] experienced a sharp decrease, implying that the rate of electron transfer increased further upon incorporation of Rd, due to its phytochemicals that act as diffusional electron mediators. On the other hand, when the Gr/f-MWCNTs/(Rd-GLD)/GOx electrode [R_{ct} 138.6 Ω, Fig. 4B (d)] or Gr/f-MWCNTs/(Rd- GLD)/HRP [R_{ct} 143.2 Ω, Fig. 4B (e)] were exposed to the same solution, a contradictory behaviour i.e., increase in R_{ct} was observed owing to the insulating property of the enzyme that impedes the electron transfer of the redox probe towards the electrode surface thus signifying the successful immobilization of the enzyme. This is furthermore verified by a series of circuit parameters like R_{ct}, solution resistance (R_s) and faradic capacitance (C_f) calculated by fitting the impedance data using equivalent circuit as shown in the inset of the Fig. 4B and as summarized in Table 1. Also observed in the equivalent circuit is the constant phase element Q, that has the general characteristics of double layer capacitor (C_{dl}) with momentous porosities and roughness with n-values close to 1. From the Fig. 4B inset we also notice the absence of Warburg component which indicates that neither Rd nor the electrode components act as a characteristic ion transport blocking membrane. The effective surface area of the modified electrodes was determined using Randle's-Sevick equation given by

$$I_p = (2.69\times10^5) A n^{3/2} D^{1/2} \upsilon^{1/2} C \qquad (1)$$

Where I_p is the peak current of redox couple, A is the effective surface area (cm^2) proportional to the value of $I_p/\upsilon^{1/2}$, n is the number of electrons participating in the redox reaction, D is diffusion co-efficient of the molecules in solution ($cm^2\ s^{-1}$), υ is the scan rate of the potential perturbation ($V\ s^{-1}$) and C is the concentration of probe molecule (mM). From equation (1) the effective surface area of Gr/f-MWCNTs/(Rd-GLD)/GOx and Gr/f-MWCNTs/(Rd-GLD)/HRP electrodes were found to be 5.32 and 5.17 cm^2 respectively

indicating that the surface area of the modified electrodes was increased much larger than that of the bare Gr electrode (0.05 cm^2).

3.4 Determination of thickness of modifying layers with EQCM

The EQCM was used to investigate the thickness of the modifying layers by monitoring the mass change. The technique can be used to detect the electrode mass change down to the nanogram level corresponding to the sub-monolayer modification. The experiments were carried out using unmodified and modified gold electrode uniformly coated with f-MWCNTs, Rd-GLD and enzyme (GOx/HRP) layers. The decrease in the frequency (or mass change) recorded in the EQCM during each step of modification was consistent with the increase in voltammetric peak current (Figure not given). The frequency of oscillation of the quartz crystal is partially dependent on the thickness of the crystal. At standard conditions, the influencing variables remain constant while a change in thickness corresponds to a change in frequency. As mass is increased on the surface of the crystal, the frequency of oscillation decreases and accordingly the thickness increases. From the change in frequency, the change in the mass of the modified layer can be calculated by the Sauerbrey equation given by

$$\text{Mass change } (\Delta m) = -1/2\ (f_o^{-2})(\Delta f)A(K\rho)^{1/2} \qquad (2)$$

Where f_o is the oscillating frequency, Δf is the change in frequency, A is the area of the gold disk coated onto the crystal, K is the shear modulus of quartz and ρ is the density of the crystal. However, a 1-Hz frequency change is equivalent to 1.4 ng of mass change. Therefore the mass change in f-MWCNTs, Rd-GDH, GOx and HRP was found to be 2.43µg, 3.8 µg, 4.12 µg and 4.13 µg respectively.

3.4 Comparisons of voltametric responses of the modified electrodes towards glucose and hydrogen peroxide detection

To scrutinize the function of Rd immobilizing matrix, the electrochemical behaviour of the different modified electrodes in the presence of 6 mM glucose has been investigated in the potential range of −0.8 to 0 mV at a scan rate of 50 mV in 0.1 M PBS. Fig. 5 shows the CVs of Gr/GOx, Gr/f-MWCNTs, Gr/f-MWCNTs/GOx and Gr/f-MWCNTs/(Rd-GLD)/GOx. The Gr/GOx electrode (Fig. 5 a) did not show any essential voltammetric response to glucose in the scanned potential range due to its inefficient ability to catalyze glucose. While, under the same potential scan, the Gr/f-MWCNTs electrode (Fig. 5 b) showed a slight increase in the magnitude of electrochemical response which can be assigned to f-MWCNTs, that increases the surface area of the electrode. The anodic peak at -0.1 V is probably due to the hydrogen adsorption behaviour of the electrode.[39] In comparison, the Gr/f-MWCNTs/GOx electrode (Fig. 5 c) showed a redox couple at −0.261 V and −0.554 V defined as anodic and cathodic peak potentials respectively and a good catalytic response to glucose. This indicates the electrochemical behaviour of the f-MWCNTs in promoting electron communication between the enzyme and the electrode[40] thus catalyzing the glucose present in the analyte. However, the catalytic response of Gr/f-MWCNTs/GOx was very small when compared to Gr/f-MWCNTs/(Rd-GLD)/GOx (Fig. 5 d) which showed ~2 times the higher current response and reasonably impressive CVs as compared with the other modified electrodes. Furthermore, the ΔE_p on the Gr/f-MWCNTs/GOx was relatively large (~70 mV) suggesting that the proposed biosensor has good electrochemical reversibility. The enhanced performance of the Gr/f-MWCNTs/(Rd-GLD)/GOx electrode towards detection of glucose is mainly attributed to the presence of biologically active constituents in Rd like polyphenols that increase the electron transfer kinetics and good biocompatibility of Rd, apparently increasing the background current.[36]

A similar effect was observed while investigating the electrocatalytic activity of HRP modified electrodes. Fig.5 inset, shows the CVs of (a) Gr/HRP, (b) Gr/f-MWCNTs, (c) Gr/f-MWCNTs/HRP and (d) Gr/f-MWCNTs/(Rd-GLD)/HRP in the presence of a 6 mM H_2O_2 in PBS (pH- 7.0) at a scan rate of 50 mV s^{-1}. The Gr/HRP showed poor electrochemical response to H_2O_2, whereas the Gr/f-MWCNTs electrode demonstrated an increased reduction peak current due to the presence of f-MWCNTs. When HRP was cast along with f-MWCNTs devoid of Rd matrix, it showed an increase in the reduction peak current in the same concentration of indicating that f-MWCNTs promotes electron transfer. Obviously, Gr/f-MWCNTs/(Rd-GLD)/HRP (curve d) demonstrated a remarkable increase in reduction current for H_2O_2 which is 4 times higher than the Gr/HRP which can be attributed to the phytochemicals of the Rd leaf that showed excellent electron transfer ability limiting the use of electron mediators thus preventing the tedious fabrication procedure required for the co-immobilization of enzyme and electron mediators. Therefore Rd may be an ideal bio-platform for enzyme immobilization and can provide a biocompatible microenvironment. The higher electrochemical response of the Gr/f-MWCNTs/(Rd-GLD)/HRP electrode towards H_2O_2 showed that it can be used for the detection and determination of H_2O_2. Further, to authenticate the electrocatalytic activity of modified electrode, CVs were recorded at different concentrations of H_2O_2 as shown in the inset (b) of Fig. 6.

In addition the surface coverage concentration (Γ) of GOx and HRP on the modified electrodes were calculated using the following equation[41]

$$\Gamma = Q/nFA \qquad (3)$$

Where Q signifies charge, n is the electron transfer, F is the Faraday constant and A is the area of the electrode. From the equation (2) the Γ of Gr/f-MWCNTs/(Rd-GLD)/GOx and Gr/f-MWCNTs/(Rd-GLD)/HRP was found to be 2.6×10^{-8} mol cm^{-2} and 7.42×10^{-8} mol cm^{-2} respectively in contrast to the f-MWCNTs alone modified GOx biosensor (2.2×10^{-8} mol

cm^{-2}) and HRP biosensor (5.41×10^{-8} mol cm^{-2}) illustrating the large enzyme loading on Rd leaf matrix.

3.5 Electrocatalytic properties of glucose biosensor

To demonstrate that the Gr/f-MWCNTs/(Rd-GLD)/GOx electrode retains its catalyzing activity, CVs were recorded with increasing concentration of glucose under oxygen saturated condition. It can be seen from the Fig. 6 that upon successive addition of 1 mM glucose to air saturated buffer solution, the reduction peak decreases because of oxygen consumption at the electrode surface. This can be explained due to the following reaction occurring in the vicinity of the electrode surface

$$\text{GOx-FAD} + \text{Glucose} \longrightarrow \text{GOx-FADH}_2 + \text{gluconolactone} \quad (4)$$

$$\text{GOx-FADH}_2 + \text{O}_2 \longrightarrow \text{GOx-FAD} + \text{H}_2\text{O}_2 \quad (5)$$

When glucose is added to the air saturated PBS, the dissolved oxygen functions as an electron acceptor and mediates the enzymatic oxidation of glucose by means of GOx. As a result, the consumption of oxygen at the electrode surface makes the reduction of the oxidized GOx less encouraging consequently leading to the decrease of the reduction in peak current and determination of glucose concentration. The inset (a) of Fig. 6 is the calibration plot of I_{pc} vs. glucose concentration which exhibits that the decrease in current is linearly proportional to the concentration of glucose up to 10 mM with a linear regression equation as shown below

$$I_p\,(\text{A}) = -1.107\times10^{-4} - 2.742\times10^{-6}\, C_{\text{glucose}}\,(\text{mM});\ R = 0.996 \quad (6)$$

The Gr/f-MWCNTs/(Rd-GLD)/GOx electrode thus demonstrates a promising tool for the detection of glucose which could be attributed to the biocompatibility of the immobilized GOx on Rd matrix.

For detailed electrochemical investigation, DPV gives a better peak resolution and higher sensitivity than CV. Hence, DPV was applied to prove the performance of the biosensor

towards the detection of glucose. Fig. 7A shows the well defined and stable DPVs obtained for the incremental addition of glucose at Gr/f-MWCNTs/(Rd-GLD)/GOx electrode in air saturated PBS in the potential range of 0 to −0.8 V. The resultant voltammetric reduction peak was found to decrease gradually with the increase of glucose concentration indicating the excellent electrocatalytic property of the modified electrode towards glucose. From the corresponding DPVs, a calibration plot of I_{pa} vs. glucose concentration was constructed as shown in the inset of Fig. 7A. Accordingly, the peak current was found to exhibit a linear relationship with glucose concentration in the range of 1 to 7 mM with a linear regression equation as below

$$I_p\,(\mathrm{A}) = -3.433\times10^{-4} - 1.516\times10^{-5}\,C_{glucose}\,(\mathrm{mM});\ R = 0.996 \qquad (7)$$

From these discussions, it is evident that the GOx immobilized on Rd matrix is effective as far as the detection of glucose is concerned.

To further investigate the electrochemical behaviour of immobilized GOx, the influence of scan rate on the Gr/f-MWCNTs/(Rd-GLD)/GOx electrode was characterized by CV. Fig. 8A depicts the CVs of biosensor obtained at different scan rates. From the figure, it is evident that for the increasing scan rates from 25-250 mV s^{-1}, the corresponding oxidation and reduction peak current increases with more positive and negative shifts in anodic and cathodic peak potentials respectively. Further inset (a) of Fig. 8A, illustrates the redox peak current increases in linear manner with scan rates in range from 25 mV s^{-1} to 125 mV s^{-1} with the linear regression equation as below indicating a surface controlled redox reaction.

$$I_{pa}\,(\mathrm{A}) = 3.731\times10^{-5} - (1.056\times10^{-6})\,\upsilon\ (\mathrm{V\ s^{-1}});\ R = 0.996 \qquad (8)$$

$$I_{pc}\,(\mathrm{A}) = -9.67\times10^{-5} - (-1.044\times10^{-6})\,\upsilon\,(\mathrm{V\ s^{-1}});\ R = -0.993 \qquad (9)$$

Conversely, when the scan rate was higher than 150 mV s^{-1} [inset (b) of Fig. 8A], redox peak current appears to be proportional to the square root of scan rate with the linear regression

$$I_{pa}\,(\mathrm{A}) = -3.949\times10^{-5} - (1.866\times10^{-5})\,\upsilon^{1/2}\,(\mathrm{V\ s^{-1}})^{1/2};\ R = 0.996 \qquad (10)$$

$$I_{pc}\,(\mathrm{A}) = -3.187\times10^{-5} - (-1.704\times10^{-5})\,\upsilon^{1/2}\,(\mathrm{V\ s^{-1}})^{1/2};\ R = -0.996 \qquad (11)$$

which is anticipated for diffusion controlled redox reaction. This signifies that at higher sweep rates the diffusion of glucose from the solution to electrode surface is a rate-limited reaction i.e., glucose is less adsorptive at the surface of the electrode.

3.5.1 Electrocatalytic properties of Hydrogen peroxide biosensor

Fig. 6 [inset (b)] illustrates the effect of varying concentration of H_2O_2 on modified biosensor. It can be observed from the CV that both the anodic and cathodic peak increased linearly with increasing concentration of H_2O_2 ranging from 0 to 6 mM. In the absence of H_2O_2 the electrode demonstrated a well established cathodic peak at −0.231 V and corresponding anodic peak at −0.03 V which is ascribed to the heme (Fe^{III}) and (Fe^{II}) redox couples of HRP immobilized on the Rd matrix. Upon increasing H_2O_2 concentration from 1 mM to 6 mM, there was an increase of reduction current and decrease in oxidation current, displaying obvious electrocatalytic behaviour of the electrochemical biosensor towards to the reduction of H_2O_2. It can be seen that the reduction of H_2O_2 occurs at -0.2V and proceeds till -0.4 V as the potential is increased at this modified electrode. The electrocatalytic mechanism of HRP with H_2O_2 has been reported in many papers and it can be expressed as follows[42]

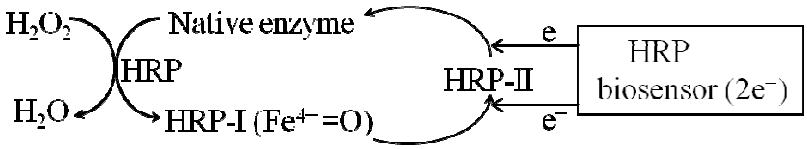

(12)

The reaction commences through oxidation of a ferriheme prosthetic group of HRP by H_2O_2 involving two electrons which results in the formation of an intermediate HRP-I (Fe^{4+}=O) which is a two-equivalent oxidized form containing an oxyferryl heme (Fe^{4+}=O) and porphyrin π cation radical. HRP-I shows catalytic activity and its porphyrin radical abstracts one electron from the electrode to form a second intermediate HRP II. The latter in turn

accepts an electron from the second donor and the enzyme is returned to its native state. The overall reaction would be

$$H_2O_2 + 2e^- + 2H^+ \longrightarrow 2H_2O \qquad (13)$$

The electrocatalytic calibration curve for the Gr/f-MWCNTs/(Rd-GLD)/HRP electrode shows a linear regression equation as follows-

$$I_{pc}\,(A) = -1.560 - (-0.029)\, C_{H2O2}\,(mM);\ R = -0.994 \qquad (14)$$

As mentioned earlier DPV is a pulse technique which allows much higher sensitivity as compared to CV. The DPVs (Fig. 7B) were scanned in the cathodic potential range from 0 V to –1 V. When the H_2O_2 concentration was increased the peak current response increased correspondingly. This result added support to CV studies demonstrating the good catalytic activity of Gr/f-MWCNTs/(Rd-GLD)/HRP. The modified electrode showed a wide linear range (inset of Fig. 7B) of H_2O_2 concentration from 0 to 7 mM with linear regression equation is as follows:-

$$I_p\,(A) = -2.350\times10^{-4} - (-2.526\times10^{-5})\, C_{H2O2}\,(mM);\ R = -0.994 \qquad (15)$$

Furthermore, the Gr/f-MWCNTs/(Rd-GLD)/HRP electrode was examined for different scan rate from 25 mV to 250 mV in PBS pH 7.0 containing 4 mM H_2O_2. It is quite evident from Fig. 8B that when the scan rate was increased the redox peak current also increased and there was a shift in the potential for each scan rate. The anodic and cathodic peak current is found to be linearly proportional to the square root of scan rate (Fig. 8B inset) representing that the electrochemical reaction occurring at Gr/f-MWCNTs/(Rd-GLD)/HRP electrode is a diffusion controlled process. The linear regression equation was found to be

$$I_{pa}\,(A) = -6.576\times10^{-5} - (2.062\times10^{-5})\, v^{1/2}\,(V\ s^{-1})^{1/2};\ R = 0.998 \qquad (16)$$

$$I_{pc}\,(A) = 7.944\times10^{-5} - (-2.588\times10^{-5})\, v^{1/2}\,(V\ s^{-1})^{1/2};\ R = -0.997 \qquad (17)$$

3.6 Influence of applied potential, pH and temperature on Gr/f-MWCNTs/(Rd-GLD)/GOx biosensor

To improve the performance of the biosensor, various influential factors such as operating potential, the pH of the supporting electrolyte and operating temperature were examined after which most favourable values were selected for subsequent experiments.

The effect of applied potential on the amperometric response of the biosensor was investigated and the outcome is exemplified in Fig. 9A. The figure demonstrates the response current of Gr/f-MWCNTs/(Rd-GLD)/GOx as a function of applied potential which was stepped from −0.3 V to −0.6 V with 0.05 V increment under constant glucose concentration (2 mM) at pH 7. It was found that the current response increased with increasing applied potential from −0.3 V to −0.45 V. This signifies that the response of the enzyme electrode was controlled by electrochemical methods. However, when the applied potential is further stepped up from −0.45 V to −0.6 V the current response decreased considerably. The maximum response was achieved at −0.45 V and it was selected as the working potential taking into consideration that at high operating potential various electroactive species like ascorbic acid and uric acid can interfere with glucose detection. This applied potential was superior to −0.49 V for graphene-GOD-PFIL electrode.[43]

Analysis of the effect of pH value on biosensor performance is of great importance because the enzyme activity is strongly affected by solution pH and extreme pH will result in denaturation of enzymes. The effect of pH on Gr/f-MWCNTs/(Rd-GLD)/GOx electrode was evaluated over the pH range from 3 to 10 by measuring the current response to 4 mM glucose. In Fig. 9B, the relationship between anodic peak current (a) and cathodic peak current (b) response to glucose with varying pH is illustrated. It displays the highest current response at pH 6. As depicted in Fig. 9B(a and b) when the pH value is increased from 3 to 6 the redox peak current seems to increase then decreases as pH increases further from 6 to 10.

It is known that for the free GOx, when oxygen is used as electron acceptor the optimum pH is generally between 4.8 to 6.[44] However, it is also reported the optimum pH for immobilized GOx may vary with different electrode material and the type of immobilization procedure. Consequently the optimum pH of 6 may be attributed to GOx immobilized on Rd matrix. Considering the physiologic pH, we have employed pH 7 for the electrochemical experiments.

Another experimental parameter, which is the thermal stability of Gr/f-MWCNTs/(Rd-GLD)/GOx electrode, was examined over the temperature range of 25 to 61 °C. Fig. 10A is the current response of the enzyme modified electrode at varying temperature. The response current increases gradually with the temperature up to 45 °C, reaching a maximum value. At a temperature higher than 45 °C the current response decreases rapidly which may be ascribed to partial denaturation of the enzyme. The maximum response obtained at 45 °C is in good agreement with available literature[45] thus indicating that Rd matrix is favourable for the immobilization of GOx which could lead to reduced conformational freedom. The dependence of current responses to temperature in the range of 25 - 61 °C is evaluated using Arrhenius relationship[45]

$$I\,(T) = I_o \exp\,(-E_a / RT) \qquad (18)$$

Where $I\,(T)$ represent the current value at specific temperature T, I_o is the proportional factor, R is the gas constant, T is temperature in Kelvin and E_a is the activation energy. The E_a for the overall electrochemical process at Gr/f-MWCNTs/(Rd-GLD)/GOx can be determined from the slope of $\ln I$ vs. $1/T$. The Arrhenius plots exhibit two straight lines as portrayed in Fig.10A inset. This kind of result has already been reported for other glucose biosensors.[46] The E_a calculated from the slopes of the plot was found to be 11.7 kJ mol^{-1} for lower temperature and 6.5 kJ mol^{-1} for higher temperature. These values are lower than reported for glucose

oxidase immobilized biosensor.[47] Lower E_a signifies that the immobilized enzyme modified electrode has good enzyme activity. This can be attributed due to the presence of the Rd leaf extract which acts as a good immobilizing matrix holding the enzyme intact.

3.6.1 Influence of applied potential, pH and temperature on Gr/f-MWCNTs/(Rd-GLD)/HRP biosensor

The effect of applied potential on Gr/f-MWCNTs/(Rd-GLD)/HRP electrode was examined in the potential range from 0 to −500 mV. Fig 9A inset shows the dependence of the current response of the biosensor on the applied potential. The current response increased gradually with an applied potential up to −350 mV. This was chosen as the applied potential for our later chronoamperometric studies.

The effect of pH on Gr/f-MWCNTs/(Rd-GLD)/HRP electrode was studied using 0.1 M PBS containing 2 mM H_2O_2. As shown in Fig. 9B (c and d) with increase in solution pH from 3 to 7 the current response of redox peaks increased linearly. When increased further the current response decreased. This may be because of elevated activity of HRP in slight alkaline solution. The maximum enzyme activity was observed at pH 7. This is similar to the results of HRP based biosensors. This also indicates that the Rd immobilizing matrix did not alter the activity of the enzyme.

In addition, the effect of temperature on the Gr/f-MWCNTs/(Rd-GLD)/HRP electrode was investigated in the temperature range from 24-44 ºC. The response gradually increased from 24 ºC up to 36 ºC after which it starts decreasing. The maximum activity was observed at 36 ºC as shown in Fig. 10B. The decrease in enzyme activity at higher temperatures is due to deactivation of enzyme. Besides, the activation energies calculated from the slopes of the two lines were found to be 12.58 kJ mol^{-1} and 2.62 kJ mol^{-1} for lower and higher temperature respectively. This E_a is smaller than 13.8 kJ mol^{-1} reported for HRP based biosensor[48]

however the E_a calculated at higher temperature is in good agreement with what has been reported for HRP based biosensors.[49]

3.7 Chronoamperometric responses of the Gr/f-MWCNTs/(Rd-GLD)/GOx and Gr/f-MWCNTs/(Rd-GLD)/HRP

Chronoamperometry is a sensitive technique used to determine biosensor characteristics such as response time, calibration curve, sensitivity, specificity and detection limit. Amperometric detection of glucose was performed with the glucose biosensor to record the change in current as a function of time at a constant potential of −450 mV in stirred condition. A stable and fast current response of less than 5s was observed with following successive injection of increasing concentration of glucose. The change in current response was linear with a correlation co-efficient of 0.993 in the concentration range from 0.5 mM to 28.5 mM as shown in Fig. 11A. This range is ample for the determination of glucose in clinical samples. In addition, the detection limit of 0.16 μM was determined with a sensitivity of 15 μA mM^{-1} cm^{-2} which is more than gelatin-MWCNTs/GOx biosensor (2.24 μA mM^{-1} cm^{-2})[50] and MWCNT/ZnO/GOx (4.18 μA mM^{-1} cm^{-2}).[51] An analysis of data in Table 2 presents the analytical results highlighting the advantages of our biosensor over other GOx based electrochemical biosensors reported in available literature.[52-55]The apparent Michaelis Menten constant K_M^{app} which is a reflection of both enzyme affinity and ratio of microscopic kinetic constant was used to evaluate the biological activity of immobilized enzymes using the electrochemical version of the Lineweaver-Burk equation[54]

$$1/I_{ss} = 1/I_{max} + K_M^{app}/I_{max}.1/c \qquad (19)$$

Where I_{ss} is the steady-state current after the addition of substrate, c is the bulk concentration of the substrate and I_{max} is the maximum current measured under saturated substrate condition. Accordingly, the K_M^{app} value for Gr/f-MWCNTs/(Rd-GLD)/GOx electrode

determined by the analysis of slope and intercept for the plots of the reciprocals of current vs. glucose concentration was found to be 1.1 mM which was smaller than 2.7 mM[52] and 2.2 mM[55] for GOx immobilized electrode giving clear evidence for the successful orientation of enzyme molecules on Rd matrix and also high affinity of our modified electrode towards glucose.

Correspondingly, Fig. 11B shows the typical current response of Gr/f-MWCNTs/(Rd-GLD)/HRP for varying concentration of H_2O_2 (0.2 mM to 6.8 mM) at an applied potential of −350 mV. The electrode reached a maximum steady state current in less than 3 s. This less response time indicates that the electrode posses good electrocatalytic activity. The calibration curve of the H_2O_2 as shown in Fig.11B inset showed a linear range from 0.2 mM to 6.8 mM with correlation co-efficient of −0.997. The sensitivity of the electrode was calculated to be 2.1 mA mM cm^{-2} and a detection limit of 0.01 μM. The K_M^{app} value which gives the enzyme-substrate kinetics calculated for Gr/f-MWCNTs/(Rd-GLD)/HRP biosensor was found to be 0.8 mM. This K_M^{app} is lower than those reported earlier for HRP based biosensors. It was found to be 3.69 ± 0.71 mM and 1.4 mM for HRP-Au-CPE[56] and HRP/chitosan-$NiFe_2O_4$ nanocomposite bioelectrode[57] respectively. The low K_M^{app} value indicated that the immobilized HRP has a good catalytic activity towards H_2O_2. This may be attributed to the presence of Rd which proves to be a good immobilizing matrix. Table 3 emphases the analytical data of the proposed Gr/f-MWCNTs/(Rd-GLD)/HRP electrode compared with other HRP biosensors.[58-61]

3.8 Effect of interferents on Gr/f-MWCNTs/(Rd-GLD)/GOx

Finally, the possible endogenous and exogenous electroactive compounds commonly present in the physiological samples affecting the accurate determination of glucose was examined. In this study, ascorbic acid (AA) and uric acid (UA) were used as endogenous interfering substances while acetaminophen (ACT) was used as an exogenous interfering substance. The

concentration of the interfering substances used in the present study was higher than the normal physiological concentration which is 0.1 mM, 0.5 mM and 0.1 mM for AA, UA and ACT respectively.[62] Fig.12 shows a typical current-time response curve of the Gr/f-MWCNTs/(Rd-GLD)/GOx electrode to (a) 4 mM glucose in presence of (b) UA, (c) AA and (d) ACT at a static potential of −450 mV. As can be seen, a significant current response proportional to the glucose concentration was observed while the amperometric response of the interfering electroactive species was relatively negligible. This may be attributed to the presence of anthocyannins in the plant chemical constituents that accelerates the AA degradation. These results prove that our biosensor is suitable for determining glucose containing physiological levels of AA and UA.

3.8.1 Effect of interferents Gr/f-MWCNTs/(Rd-GLD)/HRP biosensor

The purpose of this study was to prove that our modified electrode has the ability to eliminate interfering substances. The selectivity of the biosensor was tested using AA, UA and dopamine (DA) because they are commonly present in biological and food samples. Fig. 12 inset depicts the effect of these compounds on amperometric response. When 2 mM H_2O_2 (a) was added into the electrolyte, the developed biosensor produced an impressive current response, whereas there was no significant change in the peak current when 200 μM DA (b), 1 mM AA (c) and 0.5 mM UA (d) was added into the PBS solution. This may be largely attributed to the potential applied −350 mV for the study or the presence of anthocyannins.

3.9 Stability and reproducibility test for Gr/f-MWCNTs/(Rd-GLD)/GOx and Gr/f-MWCNTs/(Rd-GLD)/GOx electrode

The repeatability was evaluated by carrying out CV studies with an interval of three days upto 4 weeks by measuring the current response at a concentration of 2 mM glucose and with optimized experimental settings. It can be concluded that immobilized GOx on Rd leaf extract retains the entire initial activity for the first two weeks. Later a linear decrease in the

current response is pragmatic when the biosensor is reused, leading to a loss of 23% of the initial response after 4 weeks. This may be attributed to the fact that with the storage time the enzymes underwent partial denaturation. The results were found to be repeatable and reproducible during the activity measurements.

The functioning and storage stability of the Gr/f-MWCNTs/(Rd-GLD)/HRP electrode was also tested. The stability was conducted using cyclic voltammetry with the same experimental parameters. The electrode was kept for 4 weeks at 4 ºC in 0.1 M PBS (pH 7.0). CVs were recorded after the modification of the electrode. After 2 weeks the electrode sustained up to 90% of its initial activity. The enzyme activity decreased to 50% of its initial activity after 4 weeks. This long term stability can be attributed to the presence of the Rd leaf extract on electrode as visually observed and does prove to be a good immobilizing matrix.

3.10 Real Sample Analysis

The potential practical applicability of the proposed biosensors has been substantiated through real sample analysis. A standard colorimetric method with 3, 5 dinitrosalicylic acid (DNS) assay was used as a reference method to detect the concentration of glucose. 1 mL of the coconut water was mixed with 2 mL of DNS reagent. The reaction solution was heated in a water bath for 15 min and the absorbance was recorded at 540 nm. This assay showed the presence of 7.08 mg mL^{-1} glucose in the coconut water which is close to the reported value 7.25 mg $mL^{-1}$of glucose.[63] The Gr/f-MWCNTs/(Rd-GLD)/GOx biosensor was then used to estimate glucose concentration in tender coconut water using DPV in the potential range 0 to −0.8 V. The modified electrode showed good electrocatalytic response to glucose present in the coconut water. The linear response to the glucose was in the concentration range 1 to 5 mM. Further, from the standard calibration curve the amount of added glucose, found glucose, recovery and RSD was calculated and the results are summarized in Table. 4a. From

the table, it is apparent that the proposed biosensor showed an admirable recovery for glucose detection in coconut water.

In addition, an analysis of glucose in *Eleusine coracana* wine was also done using Gr/f-MWCNTs/(Rd-GLD)/GOx electrode. For this purpose, the glucose concentration of *Eleusine coracana* wine prepared in our laboratory was subjected to standard colorimetric method with 3,5 dinitrosalicylic acid (DNS) analysis. 1 mL of the wine was mixed with 2 mL of DNS reagent and the absorbance of the resulting solution was recorded at 540 nm. The results calculated from the standard calibration curve of glucose using the DNS method demonstrated the presence of 0.96 mg mL^{-1} of glucose. Then, the analyte concentration in the wine was estimated electrochemically using the modified electrode. Table 4a shows the results for the biosensor which is in good concurrence with the added amount of the glucose in the wine. The recovery of the glucose was in the range of 103-106% and the relative standard deviations (RSD) were in the range of 1.2-9.3%. This proves the excellent practical applicability of the biosensor for the determination of glucose in wine.

Subsequently, we examined the ability of Gr/f-MWCNTs/(Rd-GLD)/HRP in determining the H_2O_2 concentration in herbal bleach because it is often used in many cosmetics used daily. The herbal bleach was labelled to contain 3% H_2O_2. The H_2O_2 content in the sample was determined with the Gr/f-MWCNTs/(Rd-GLD)/HRP electrode by an amperometric method. The operating potential was kept static at −350 mV. The modified electrode showed a good linear range from 2 to 5 mM with a correlation co-efficient of −0.988. Upon repetitive spiking of the local brand of herbal bleach, the biosensor yielded the results as summarized in Table 4b. The RSD was in the range 1.63-2.95 % and the recovery in the range of 97.5-108% which were acceptable, indicating the viability of the biosensor to determine H_2O_2 in the commercial sample.

4. Conclusion

In conclusion, we have proposed Rd leaf as a novel, economic and natural immobilizing matrix for immobilization of GOx and HRP. The added advantage of Rd leaf is that it contains many phytochemicals like anthocyanins which act as counters for interfering substances and polyphenols that on oxidation produce quinones which generally increase the kinetics of electron transfer. SEM and EDX images have provided a morphological characterization which complements the results obtained by CV, DPV and chronoamperometry. The proposed biosensors Gr/f-MWCNTs/(Rd-GLD)/GOx and Gr/f-MWCNTs/(Rd-GLD)/HRP exhibit good linearity, stability and specificity. In this study it has been demonstrated that the developed biosensor was used in the analysis of real sample for the estimation of glucose and H_2O_2.

Acknowledgements

The authors gratefully acknowledge the financial support from the Department of Atomic Energy – Board of Research in Nuclear Sciences, Government of India and Vision group on science & technology, Government of Karnataka. We thank Sri. A.V.S. Murthy, honorary secretary, Rashtreeya Sikshana Samiti Trust, Bangalore and Dr. Shanta Sastry, Principal, N.M.K.R.V. College for Women, Bangalore for their continuous support and encouragement. We also thank Prof. N. Manu Chakravarthy for his valuable suggestions in writing of this manuscript. Sangaraju Shanmugam thanks the Ministry of Education, Science and Technology of Korea for supporting the R & D Programme (13-BD-01) to DGIST.

References

1 J.X. Wang, X.W. Sun, A. Wei, Y. Lei, X.P. Cai, C.M. Li and Z.L. Dong, *Appl. Phys. Lett*., 2006, **88**, 233106-233108.

2 S. Nandini, S. Nalini, R. Manjunatha, S.S. Shanmugam , J.S. Melo and G.S. Suresh, *J. Electroanal. Chem*., 2013, **689**, 233-242.

3 R. Manjunatha, D. H. Nagaraju, G.S. Suresh, J.S. Melo , S.F. D'Souza and T.V. Venkatesha, *J. Electroanal. Chem*., 2011, **651**, 24-29.

4 E.C. Hurdis and H. Romeyn, *Anal. Chem*., 1954, **26**, 320-325.

5 M.C.Y. Chang, A. Pralle, E.Y. Isacoff and C.J. Chang, *J. Am. Chem. Soc*., 2004, **126**, 15392-15393.

6 C. Matsubara, N. Kawamoto and K.Takamura, *Analyst* 1992, **117**, 1781-1784.

7 K. Nakashima, K. Maki, S. Kawaguchi, S.Akiyma, Y. Tsukamoto and I. Kazuhiro, *Anal. Sci*.,1991, **7**, 709-713.

8 Y. Song, L.Wang, C.Ren, G.Zhua and Z.Li, *Sens. Acutators B*, 2006, **114**, 1001-1006.

9 L.C. Clark and C. Lyons, *Ann. New York Acad. Sci*., 1962, **102**, 29-45.

10 M. Nanjo and G.G. Guilbault, *Anal. Chim. Acta*., 1974, **73**, 367-373.

11 S.J. Updike and G.P. Hicks, *Nature*, 1967, **214**, 986-988.

12 J. Raba and H.A. Mottol, *Crit. Rev. Anal. Chem*., 1995, **25**, 1-42.

13 L. Gorton, A. Lindgren, T. Larsson, F.D. Munteanu, T. Ruzgas and I. Gazaryan, *Analytica Chimca Acta*, 1999, **400**, 91-108.

14 G. Jonsson and L. Gorton, *Electroanalysis*, 1989, **1**, 465-468.

15 M.E.G. Lyons and G.P. Keeley, *Int. J. Electrochem. Sci*., 2008, **3**, 819-853

16 H. Korri-Youssoufi, N. Desbenoit, R. Ricoux, J.P. Mahy and S. Lecomte, *Mater. Sci. Eng. C*, 2008, **28**, 855-860.

17 T. Zhang, B. Tian, J. Kong, P. Yang and B. Liu, *Anal. Chim. Acta*, 2003, **489**, 199-206.

18 S. Campuzano, B. Serra, M. Pedrero, F.J. Villena and J.M. Pingarron, *Anal. Chim. Acta*, 2003, **494**, 187-197.

19 E. Dempsey, D. Diamond and A. Collier, *Biosens. Bioelectron*., 2004, **20**, 367-377.

20 J.S. Melo and S.F. D'Souza, *Appl. Biochem. Biotechnol*., 1992, **32**, 159-170.

21 H. Elwing, *Biomaterials*, 1998, **19**, 397-406.

22 P.D. Gaikwad, D.J. Shirale, V.K.Gade, P.A.Savale, H.J. Kharat, K.P.Kakde and M.D. Shirsat, *Int. J. Electrochem. Sci*., 2006, **1**, 425-434.

23 M.M.F. Choi and T.P. Yu, *Enzyme Microb. Tech*., 34 (2004) 41-47.

24 P.E. Michel, S.M.G. Sauvigne and L.J. Blum, *Anal. Chim. Acta*, 1998, **360**, 89-99.

25 Y.Q. Zhang, *Biotechnol. Adv*., 1998, **16**, 961-971.

26 X. Yang, Z. Zhou, D. Xiao and M. M. F. Choi, *Biosens. Bioelectron*., 2006, **21**,1613-1620.

27 J. Kumar and S.F. D'Souza, *Biosens. Bioelectron*., 2009, **24**, 1792-1795.

28 S. Ijima, Nature, 1991, **354**, 56-58.

29 M. Valcarcel, B.M. Simonet, S. Cardenas and B. Zuarez, *Anal. Bioanal. Chem*., 2005, **382**, 1783-1790.

30 A.S. Adekunle, B.O. Agboola, J. Pillay and K.I. Ozoemena, *Sens. Actuartors B*, 2010, **148**, 93-102.

31 A.K. Upadhyay, T.W.Ting and S.M. Chen, *Talanta*, 2009, **79**, 38-45.

32 Y. Liu, J. Lie and H. Ju, *Talanta*, 2008, **74**, 965-970.

33 E. Idaka, T. Ogawa, T. Kondo and T. Goto, *Agri. Biol. Chem*., 1987, **51**, 2215– 2220.

34 A. Meybeck, P. Potier, F. Bonte, F.Picot and J.P. Cosson, Eur. Pat., 19980942792, 2000.

35 O. Makhotkina and P.A. Kilmartin, *J. Electroanal. Chem*., 2009, **633**, 165-174.

36 J.Wang, *Electroanal*., 2001, **13**, 983-988.

37 J. Wang, *Chem. Rev*., 2008, **108**, 814-825.

38 A. R. Munguia, E. A. Nieto, C. I. Beristain, F. C. Sosa and E. J. V. Carter, *J. Food*, 2009, **7**, 209-216.

39 C.H. Chen and C.C. Huang, *Sep. Purif. Technol*., 2009, **65**, 305-10.

40 M. Pumeraa, S. Sanchez, I. Ichinose and J.Tang, *Sens. Actuartors B*, 2007, **123**, 1195-1205.

41 Q. Xu, C. Mao, N.N. Liu, J.J. Zhu and J. Sheng, *Biosens. Bioelectron*., 2006, **22**, 768-773.

42 E. Csoeregei, L. Gorton and G. M. Varga, *Anal. Chem*., 1994, **66**, 3604-3610.

43 J.Wang, *Chem. Rev*., 2008, **108**, 814-825.

44 C. Shan, H. Yang, J. Song, D. Han, A. Ivaska and L. Niu, *Anal. Chem.*, 2009, **81**, 2378-2382

45 V.R. Sarath Babu, M.A. Kumar, N.G. Karanth and M.S. Thakur, *Biosens. Bioelectron*., 2004, **19**, 1337-1341.

46 J. R. Retama, E. L. Cabarcos and B. L. Ruiz, *Talanta*, 2005, **68**, 99-107

47 C.G.J. Koopal and R.J.M. Nolte, *Bioelectrochem. Bioenerg*., 1994, **33**, 45-53.

48 Y.F. Yang and S.L. Mu, *J. Electroanal. Chem*., 1997, **432**, 71-78.

49 J.J. Xu, G.Wang, Q. Zhang, X.H. Xia and H.Y. Chen, *Chinese Chem. Lett*., 2005, **16**, 523-526.

50 A.P. Periasamy, Y.J. Chang and S.M. Chen, *Bioelectrochemistry*, 2011, **80**,114-120.

51 S. Palanisamy, S. Cheemalapati and S. M. Chen, *Int. J. Electrochem. Sci*., 2012, **7**, 8394-8407.

52 A. Salimi, E. Sharifi, A. Noorbakhsh and S. Soltanian, *Biosens. Bioelectron*., 2007, **22**, 3146-3153.

53 Y. Liu, X. Feng, J. Shen, J.J. Zhu and W. Hou, *J. Phys. Chem. B*, 2008, **112**, 9237-9242.

54 X. Kanga, J. Wang, H. Wu, I.A. Aksay, J. Liu and Y. Lin, *Biosens. Bioelectron*., 2009, **25**, 901-905.

55 G.Wang, J.J. Xu, H.Y. Chen and Z.H. Lu, *Biosens. Bioelectron*., 2003, **18**, 335-343.

56 S.Q. Liu and H. X. Ju, *Anal. Biochem*., 2002, **307**, 110-116.

57 F. Yalciner, E. Cevik, M. Senel and A. Baykal, *Nano-Micro Lett*., 2011, **3**, 91-98.

58 S. Zong, Y. Cao, Y. Zhou and H. Ju, *Langmuir*, 2006, **22**, 8915-8919.

59 S. Xu, X. Zhang, T. Wan and C. Zhang, *Microchim. Acta*, 2011, **172**, 199-205.

60 L. Feng, L. Wang, Z. Hu, Y. Tian, Y. Xian and L. Jin, *Microchim. Acta*, 2009, **164**, 49-54.

61 Y. Miao and S.N. Tan, *Analyst*, 2000, **125**, 1591-1594.

62 B.Y. Wu, S.H. Hou, F. Yin, J. Li, Z.X. Zhao, J.D. Huang and Q. Chen, *Biosens. Bioelectron*., 2007, **22**, 838-844.

63 J.W. H. Yong, L. Ge, Y.F. Ng and S.N. Tan, *Molecules*, 2009, **14**, 5144-5164.

Figure Captions

Fig. 1 Schematic view of fabrication process of the glucose and H_2O_2 biosensors using Rd leaf extract.

Fig. 2 Typical SEM images of (A) Gr/f-MWCNTs, (B) Gr/f-MWCNTs/Rd-GLD (C) Gr/f-MWCNTs/(Rd-GLD)/GOx and (D) Gr/f-MWCNTs/(Rd-GLD)/HRP modified electrodes.

Fig. 3 EDX image of (A) Gr/f-MWCNTs, (B) Gr/f-MWCNTs/Rd-GLD (C) Gr/f-MWCNTs/(Rd-GLD)/GOx and (D) Gr/f-MWCNTs/(Rd-GLD)/HRP. Inset is the quantitative results obtained from the EDX spectra of the corresponding electrodes.

Fig. 4 (A) CVs of 5 mM $Fe(CN)_6^{3-/4-}$ solution obtained at (a) Gr/f-MWCNTs, (b) Gr/f-MWCNTs/Rd-GLD (c) Gr/f-MWCNTs/(Rd-GLD)/GOx and (d) Gr/f-MWCNTs/(Rd-GLD)/HRP. (B) The impedance spectrum of Gr/f-MWCNTs (a), Gr/f-MWCNTs/Rd-GLD (b), Gr/f-MWCNTs/(Rd-GLD)/GOx (c) and Gr/f-MWCNTs/(Rd-GLD)/HRP (d) in 5 mM $Fe(CN)_6^{3-/4-}$. Experimental fit —— Best model fit ○ ⬢ ◍ ⬠. Inset is the Randles equivalence circuit used to fit the impedance data obtained for all the modified electrodes.

Fig. 5 CVs of (a) Gr/GOx, (b) Gr/f-MWCNTs, (c) Gr/f-MWCNTs/GOx and (d) Gr/f-MWCNTs/(Rd-GLD)/GOx in presence of 6 mM glucose in 0.1 M PBS solution. Inset- CVs of (a)Gr/HRP, (b) Gr/f-MWCNTs, (c) Gr/f-MWCNTs/HRP and (d) Gr/f-MWCNTs/(Rd-GLD)/HRP in presence of 6 mM H_2O_2 0.1 M PBS solution at a scan rate of 50 mV s^{-1}.

Fig. 6 CVs of Gr/f-MWCNTs/(Rd-GLD)/GOx with addition of increasing concentration of glucose (a-j) 0 to 10 mM. Inset (a) calibration plot of peak current versus concentration of glucose. (b) CVs obtained at Gr/f-MWCNTs/(Rd-GLD)/HRP with addition of 0 to 6 mM H_2O_2 to nitrogen saturated solution.

Fig. 7 (A) Cathodic DPVs for the detection of glucose at Gr/f-MWCNTs/(Rd-GLD)/GOx electrode in 0.1 M PBS oxygen saturated solution in the concentration range (a-g) 0-7 mM. Inset is the plot of peak current vs. concentration of glucose. (B) DPVs of Gr/f-

MWCNTs/(Rd-GLD)/HRP electrode for the different concentration of H_2O_2 (a=0, b-h; 1-7 mM). Inset shows cathodic peak current vs. concentration plot of H_2O_2.

Fig. 8 (A) Different scan rate study of Gr/f-MWCNTs/(Rd-GLD)/GOx in the range of 25 mV to 250 mV (a-j). Inset (a) Plot of anodic and cathodic peak current vs. scan rate (b) Plot of peak current vs. square root of scan rate. (B) Gr/f-MWCNTs/(Rd-GLD)/HRP at different scan rates a-j (25-250 mV). Inset- linear dependence of I_{pa} and I_{pc} on square root of scan rates.

Fig. 9 (A) Effect of working potential on the Gr/f-MWCNTs/(Rd-GLD)/GOx studied by amperometry. Inset is the plot of peak current vs. varying operating potential examined at Gr/f-MWCNTs/(Rd-GLD)/HRP electrode. (B) Peak current response of Gr/f-MWCNTs/(Rd-GLD)/GOx [I_{pa} (a) I_{pc} (b)] and Gr/f-MWCNTs/(Rd-GLD)/HRP [I_{pa} (c) I_{pc} (d)] modified electrodes with varying pH from 3 to 10.

Fig. 10 (A) The current response of the glucose biosensor as a function of temperature. Inset Arrhenius plot of the data points. (B) Effect of temperature on the response of Gr/f-MWCNTs/(Rd-GLD)/HRP modified electrode with temperature ranging from 24-44 ˚C. Inset Arrhenius plot.

Fig. 11 (A) The calibration plot of current vs. concentration of glucose obtained using current-time curve at Gr/f-MWCNTs/(Rd-GLD)/GOx electrode. (B) The current-time curve of Gr/f-MWCNTs/(Rd-GLD)/HRP electrode in 0.1 M PBS at a static potential of −350 mV in presence of varying concentration of H_2O_2. Inset shows calibration plot of current against concentration of H_2O_2.

Fig. 12 Amperometric responses recorded with glucose biosensor at −450 mV upon successive additions of (a) 4 mM glucose, (b) UA, (c) AA and (d) ACT. Inset shows the effect of interferents on the Gr/f-MWCNTs/(Rd-GLD)/HRP electrode examined in presence of 2 mM H_2O_2 (a) 200 µM DA (b), 1 mM AA (c) and 0.5 mM UA (d).

Table 1 EIS data of bare Gr, Gr/f-MWCNTs, Gr/f-MWCNTs/(Rd-GDH), Gr/f-MWCNTs/(Rd-GDH)/GOx and Gr/f-MWCNTs/(Rd-GDH)/HRP

Electrode	R_s /Ω	C_{dl}/F	n	R_{ct}/Ω	C_f/F
Bare Gr	33.7	3.25×10^{-6}	0.78	184	0.00036
Gr/f-MWCNTs	118.8	0.00036	0.93	44.01	0.00046
Gr/f-MWCNTs/Rd-GDH	116.4	5.17×10^{-10}	1	16.98	0.00042
Gr/f-MWCNTs/(Rd-GDH)/GOx	123.7	0.0003	0.89	138.6	0.00037
Gr/f-MWCNTs/(Rd-GDH)/HRP	128.5	0.0020	0.82	143.2	0.0019

Table 2 Comparison of the proposed glucose biosensor with other GOx immobilized electrodes.

Electrode	Response time/s	Linear range/mM	Detection limit /μM	Sensitivity /μA mM^{-1} cm^{-2}	Reference
Gelatin-MWCNTs/GOx	-	6.30-20.09	-	2.47	52
MWCNTs/ZnO/GOx[47]	>5	0.2-27.2	20	4.18	53
GOx /NiO modified GC electrode	3	0.03-5	24	0.4	54
PS/PANI/Au/GOD/Nafion Modified electrode	10s	0.04-2.04	12	-	55
Gr/f-MWCNTs/(Rd-GDH)/GOx	>5	0.5-28.5	0.16	15	This work

Table 3 Comparison of the proposed H_2O_2 biosensor with other HRP immobilized electrodes

HRP biosensor	Response time/s	Linear range /mM	Detection limit/μM	Sensitivity /mA mM^{-1} cm^{-2}	Reference
HRP/ZrO2-grafted collagen/ DMSO/GE	< 5	1.0 – 0.073	0.25	260	58
HRP- MWNTs-GCE	2	0.00095- 9.5	0.4	-	59
CS/HRP/Fc	< 10	0.035-1.1	8.0	0.172	60
Chitosan HRP modified enzyme electrode	-	0.047-2	3	0.0187	61
Gr/f-MWCNTs/ (Rd-GDH)/HRP	< 3	0.2 - 6.8	0.01	2.1	Present work

Table 4a Determination of glucose in tender coconut water (n=5) and *Eleusine coracana* wine (n=5) with the glucose biosensor

Sample	Sl.No	Added / mM L^{-1}	Found / mM L^{-1}	Recovery (%)	RSD (%)
Coconut	1	3	3.19	106	1.5
water	2	4	4.02	100.5	1.26
	3	5	5.16	103.5	9.88
wine	4	2	2.08	104	1.2
	5	3	3.2	106	9.3
	6	4	4.14	103.5	7.2

4b Determination of H_2O_2 in herbal bleach (n=5) with the hydrogen peroxide

Sample	Sl.No	Added /mM L^{-1}	Found /mM L^{-1}	Recovery (%)	RSD (%)
Herbal	1	2	2.16	108	2.95
bleach	2	3	3.24	108	1.97
	3	4	3.9	97.5	1.63

Table of contents entry

This work aims at using non toxic, easily available *Rhoeo discolor* (Rd) leaf extract as a matrix for enzyme immobilization in the development of electrochemical biosensors.

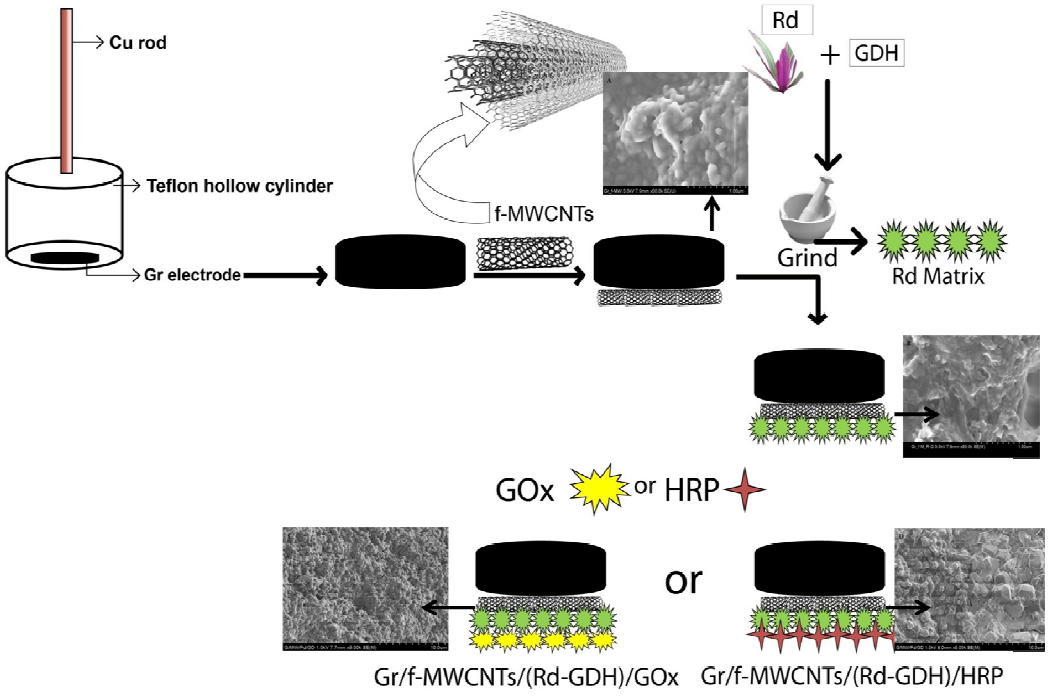

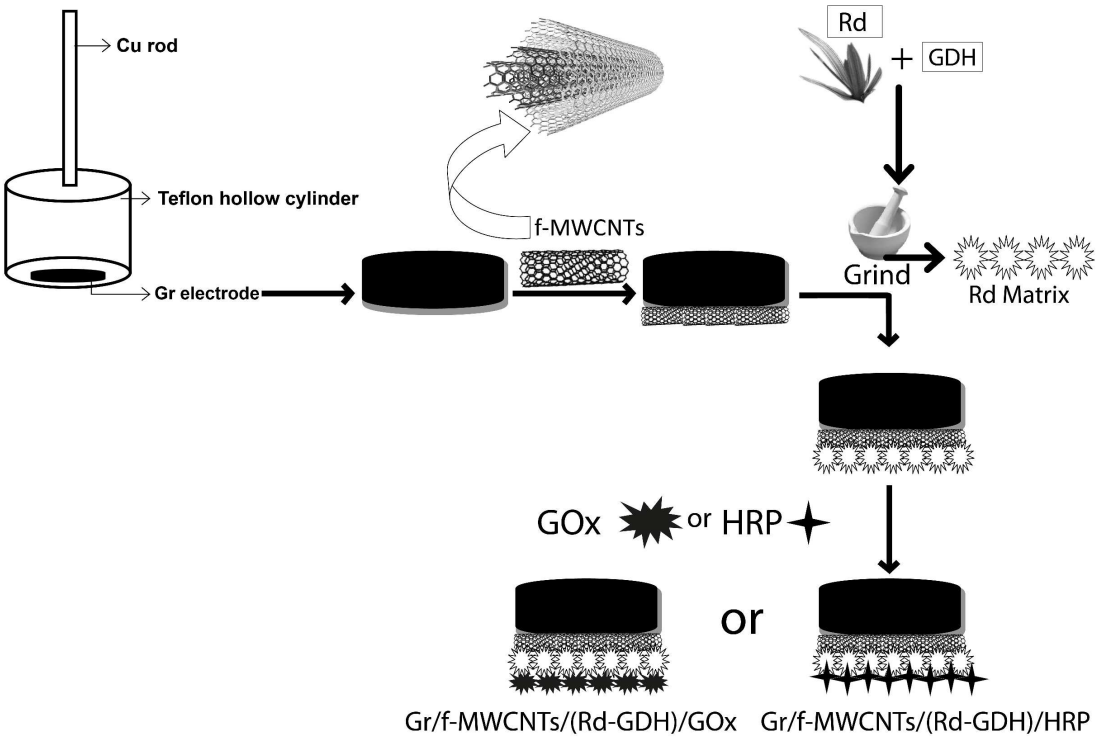

Fig. 1

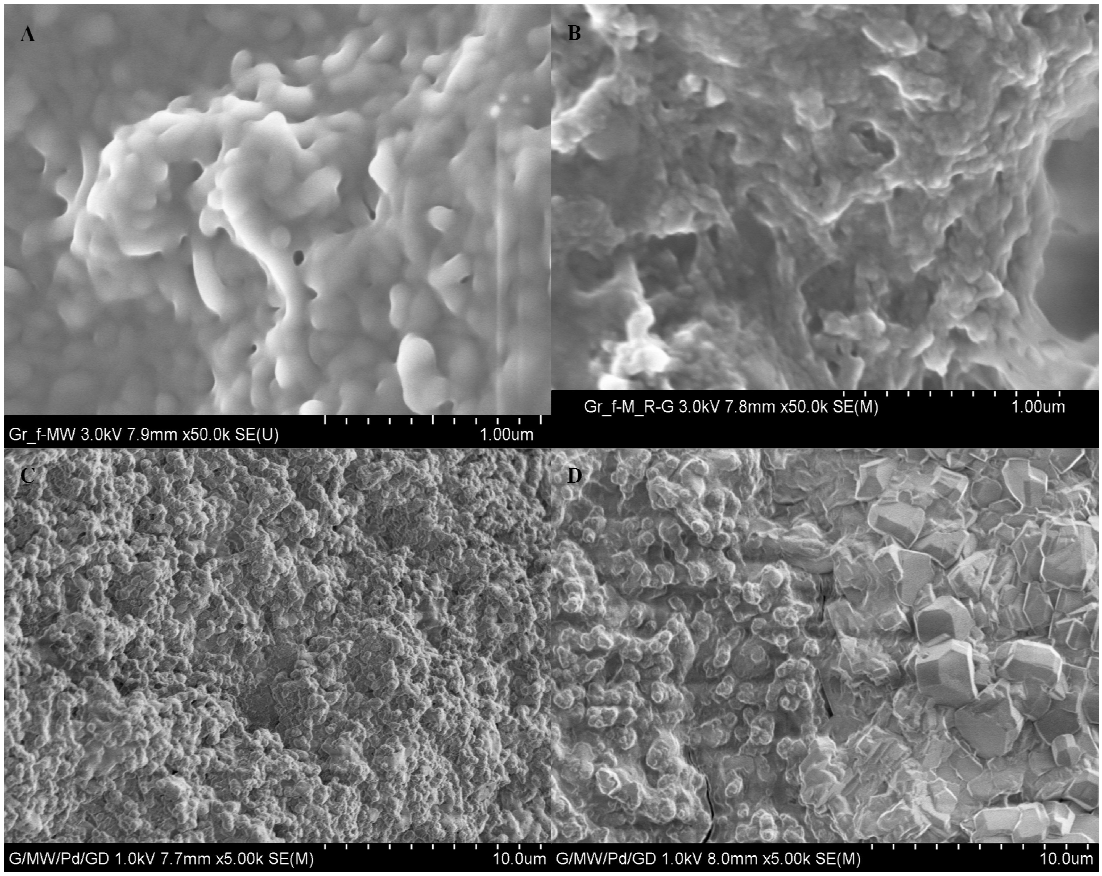

Fig. 2

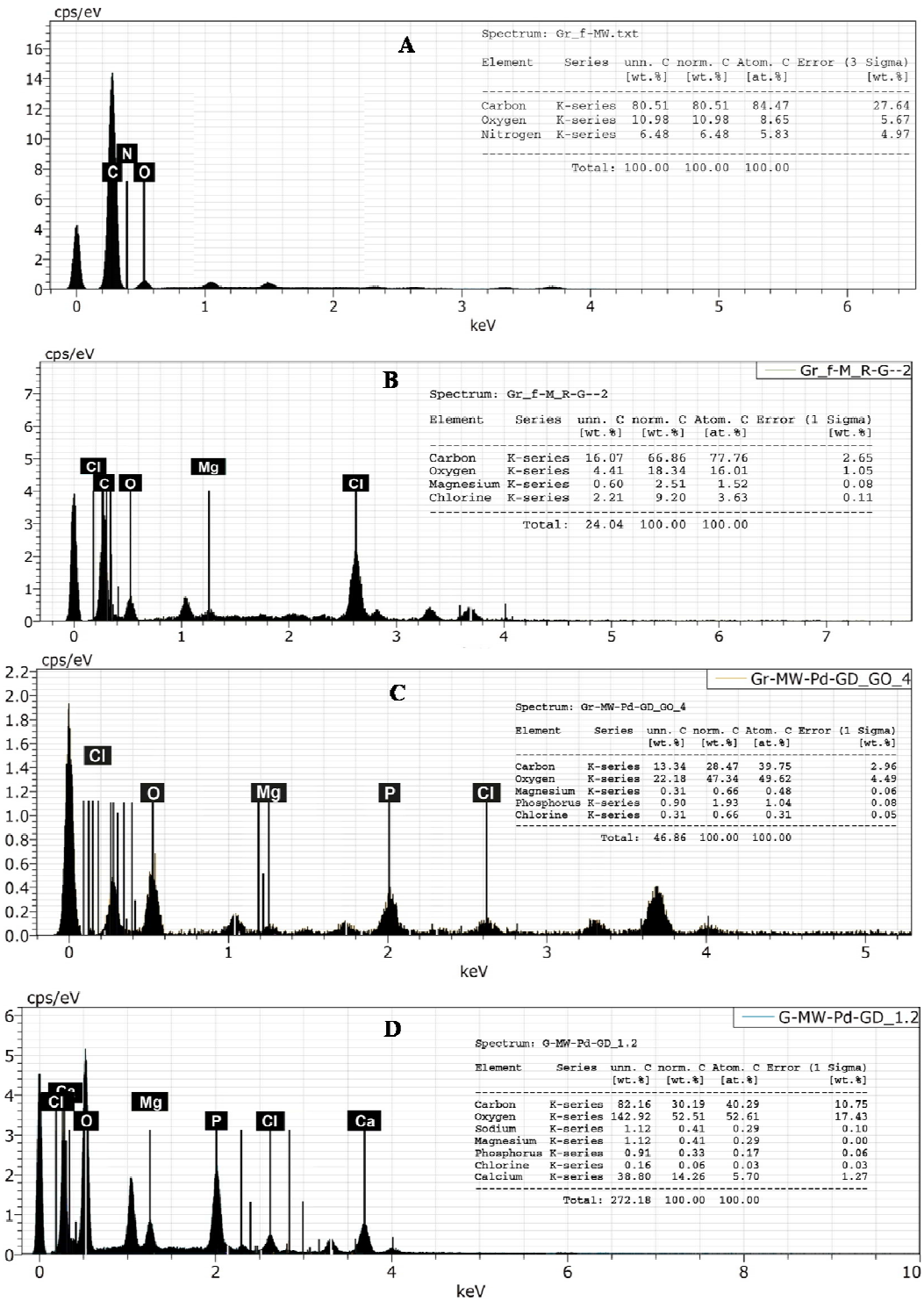

Fig. 3

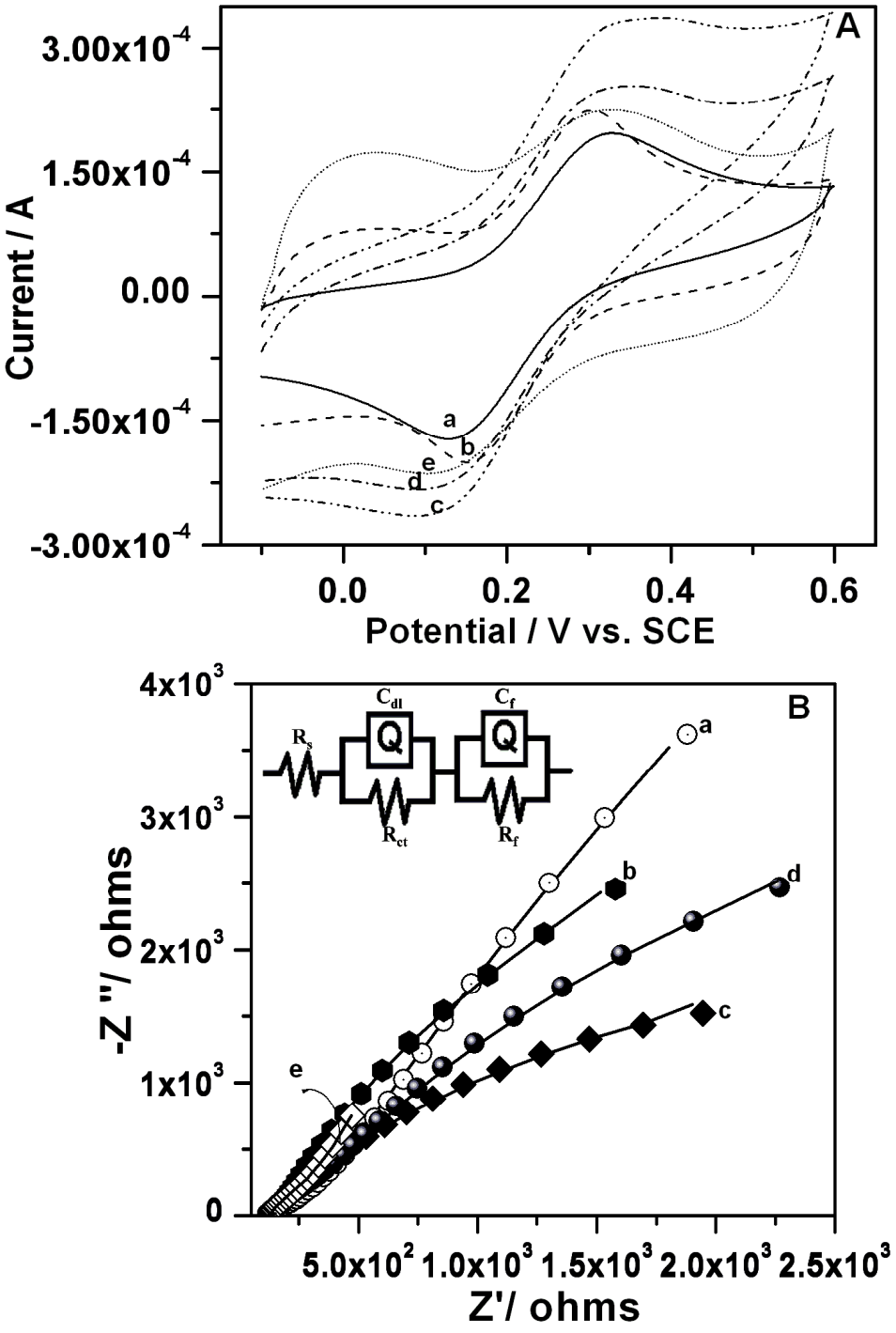

Fig. 4

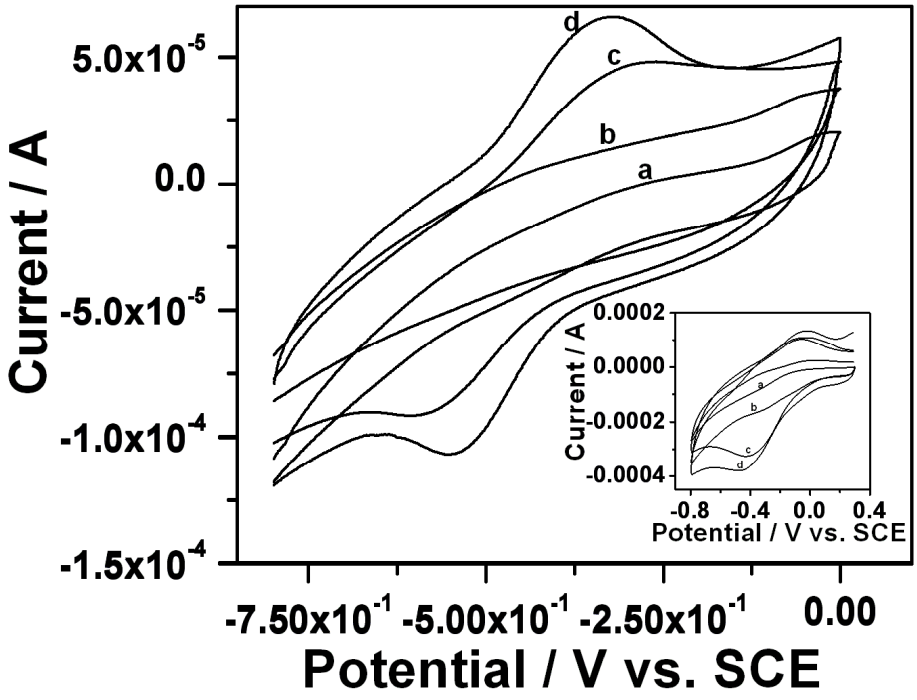

Fig. 5

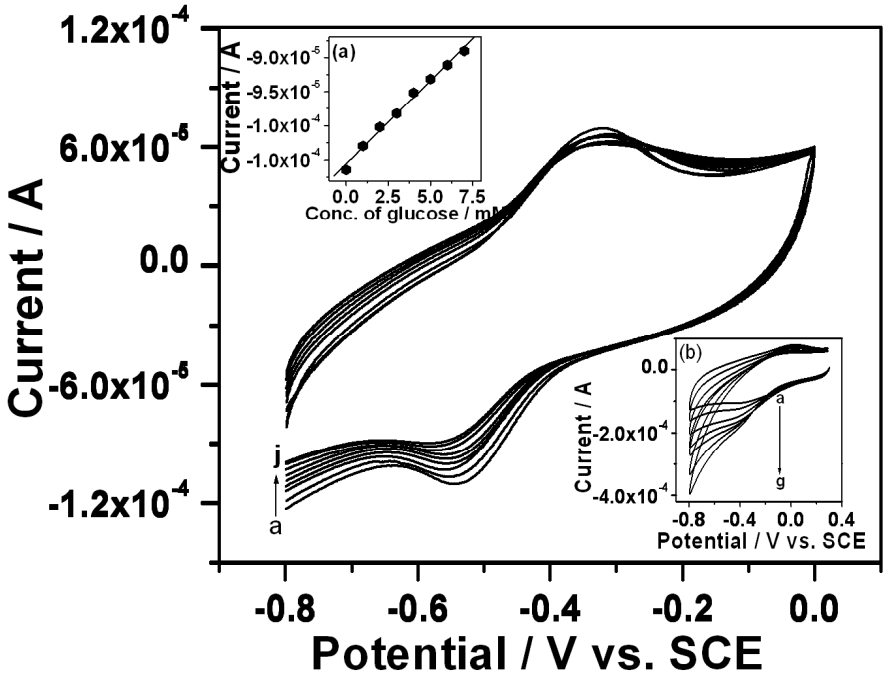

Fig. 6

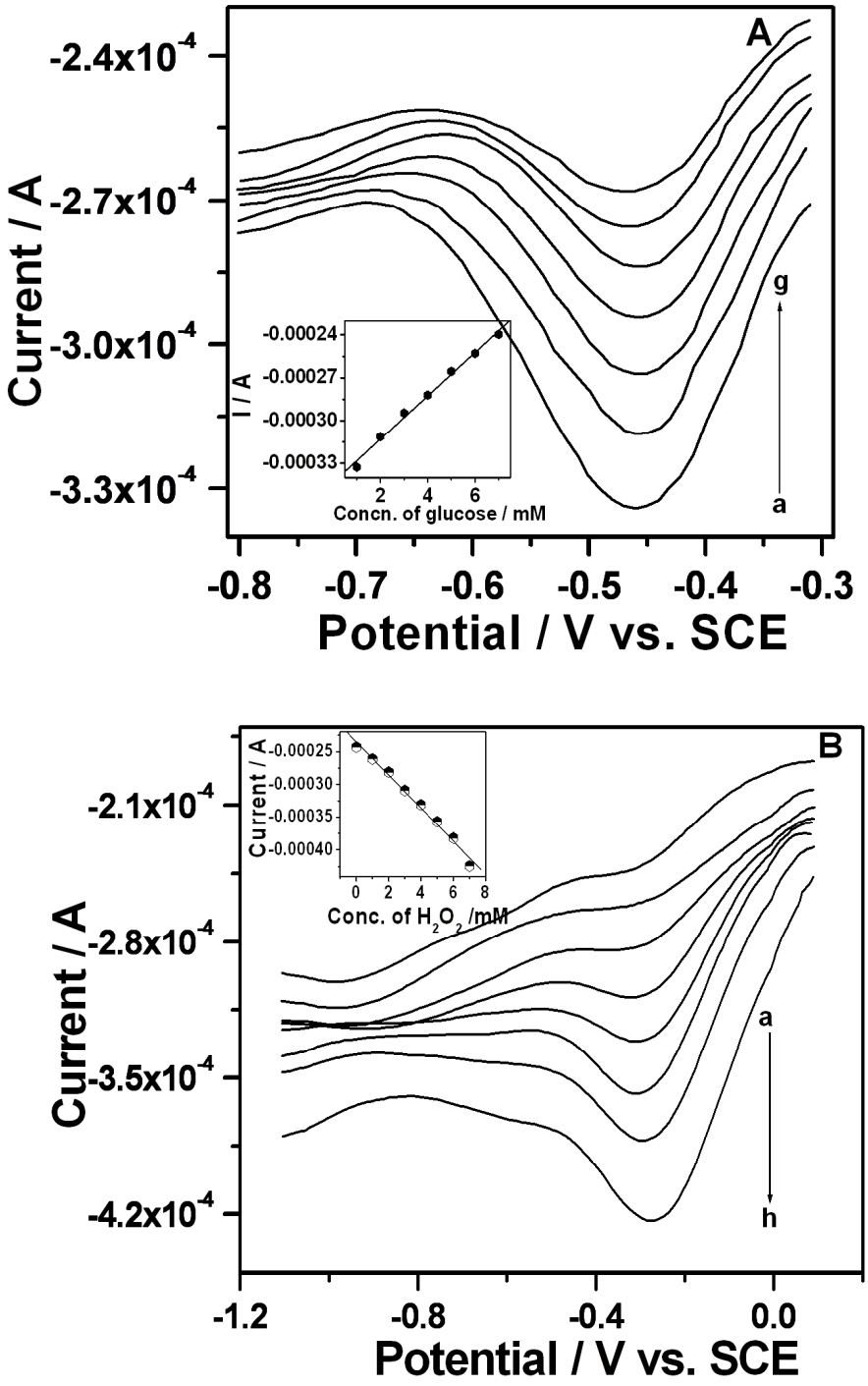

Fig. 7

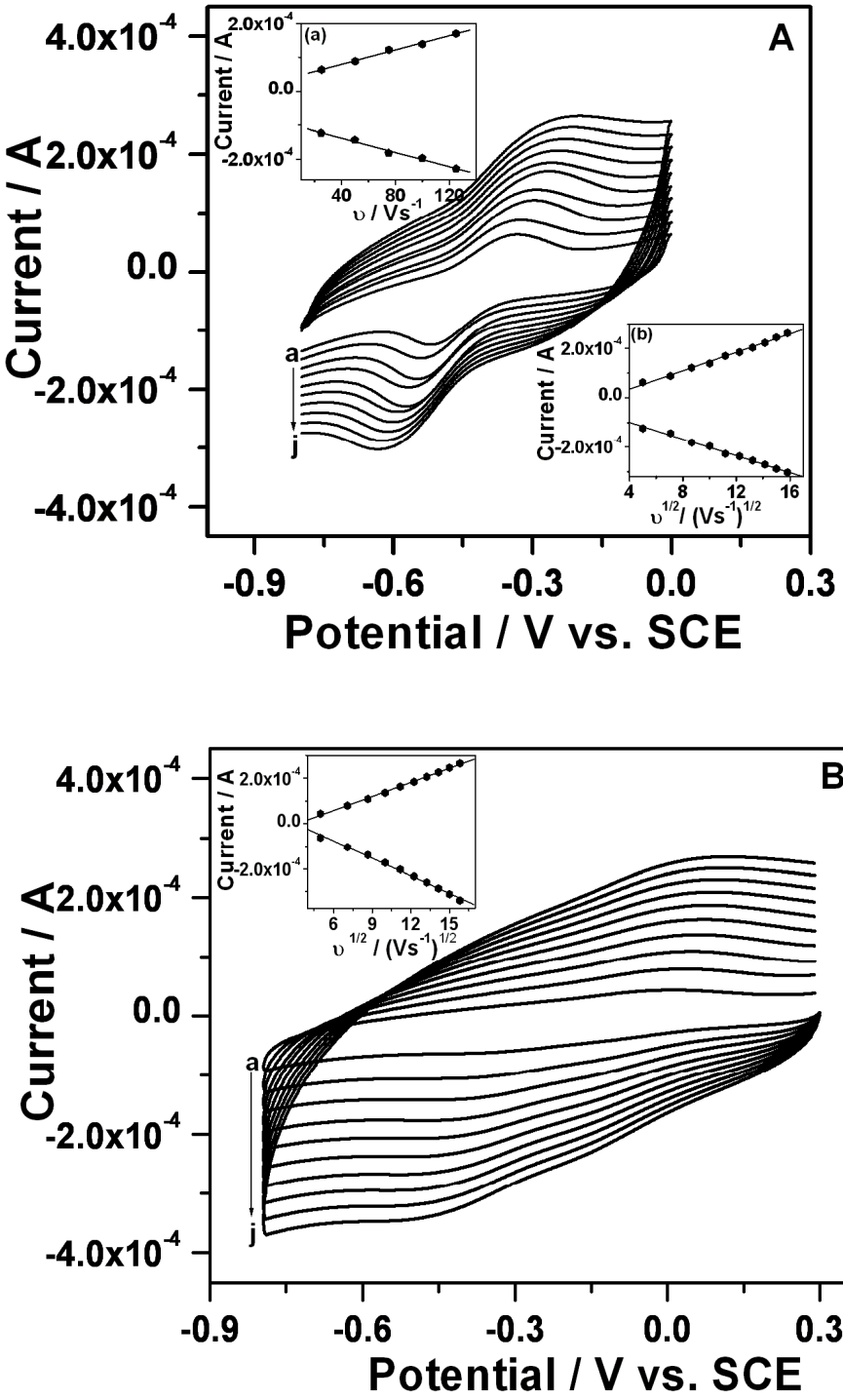

Fig. 8

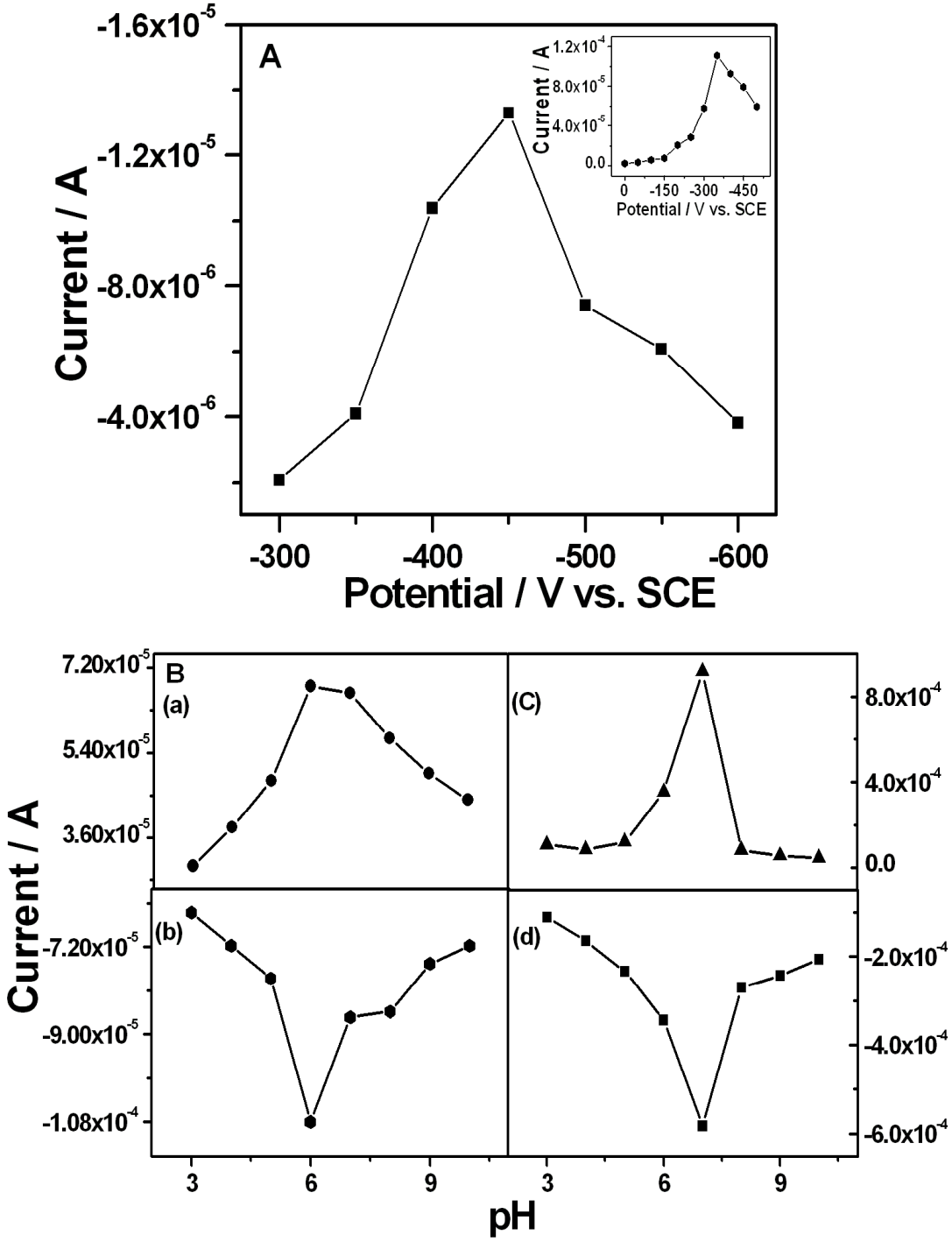

Fig. 9

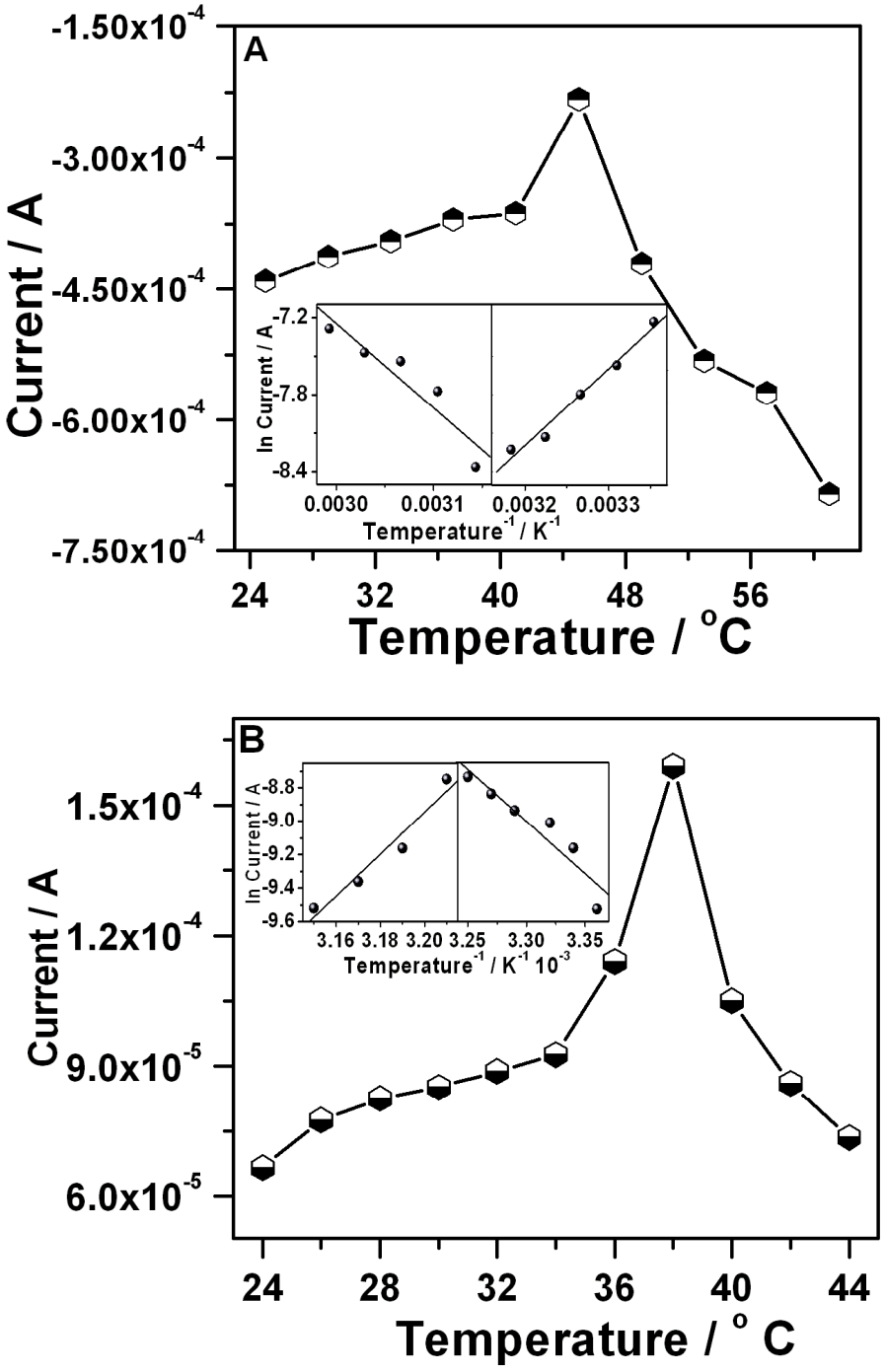

Fig. 10

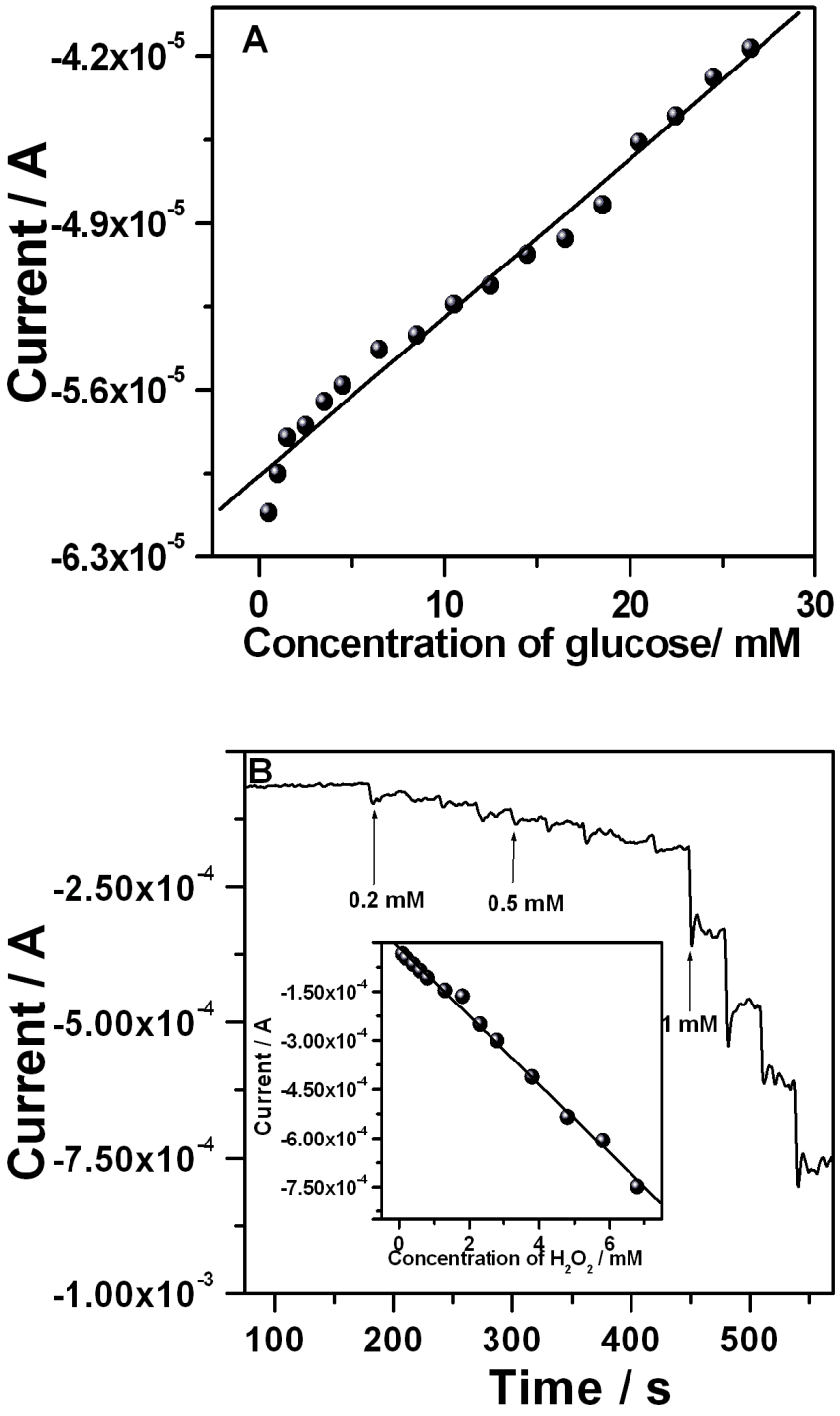

Fig. 11

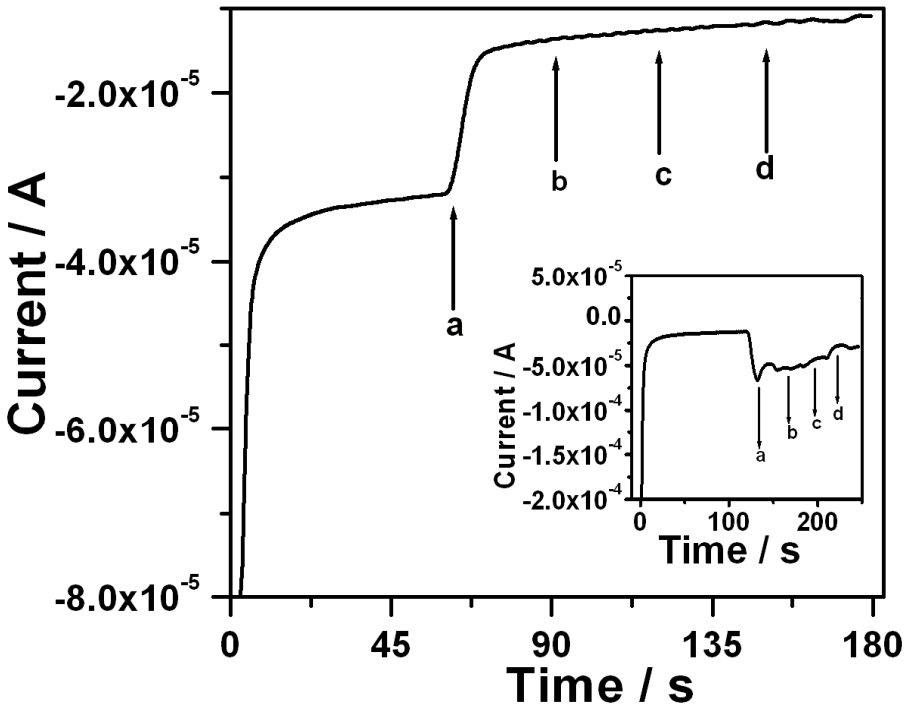

Fig. 12